ISSN 1075-7015, Geology of Ore Deposits, 2017, Vol. 59, No. 3, pp. 183–208. © Pleiades Publishing, Ltd., 2017.
Original Russian Text © V.A. Petrov, A.B. Leksin, V.V. Pogorelov, Yu.L. Rebetsky, V.A. San'kov, S.V. Ashurkov, I.Yu. Rasskazov, 2017, published in Geologiya Rudnykh Mestorozhdenii, 2017, Vol. 59, No. 3, pp. 173–200.

Geodynamic Simulation of Ore-Bearing Geological Structural Units by the Example of the Strel'tsovka Uranium Ore Field

V. A. Petrov[a], *, A. B. Leksin[a], V. V. Pogorelov[b], Yu. L. Rebetsky[b], V. A. San'kov[c], S. V. Ashurkov[c], and I. Yu. Rasskazov[d]

[a] *Institute of Geology of Ore Deposits, Petrography, Mineralogy, and Geochemistry, Russian Academy of Sciences, Moscow, 119017 Russia*
[b] *Schmidt Institute of Physics of the Earth, Russian Academy of Sciences, Moscow, 123242 Russia*
[c] *Institute of the Earth's Crust, Siberian Branch, Russian Academy of Sciences, Irkutsk, 664033 Russia*
[d] *Institute of Mining, Far East Branch, Russian Academy of Sciences, Khabarovsk, Russia*
**e-mail: Vlad243@igem.ru*

Received August 22, 2016

Abstract—Information on designing a 3D integrated model of the deflected mode (DM) of rock massif near the Strel'tsovka uranium ore field (SUOF) in the southeastern Transbaikal region is presented in the paper. This information is based on the contemporary stresses estimated by geostructural and tectonophysical techniques and by studying the seismotectonic deformation of the Earth's surface using the data on earthquake source mechanisms and GPS geodesy focused on the recognition of active faults. A combination of the results of geostructural, geophysical, geotectonic, and petrophysical research, as well as original maps of faulting and the arrangement of seismic dislocations and seismotectonic regimes (stress tensors), allowed us to design models of the structure, properties, and rheological links of the medium and to determine the boundary conditions for numerical tectonophysical simulation using the method of terminal elements. The computed 2D and 3D models of the state of the rock massif have been integrated into 3D GIS created on the basis of the ArcGIS 10 platform with an ArcGIS 3D-Analyst module. The simulation results have been corroborated by in situ observations on a regional scale (the Klichka seismodislocation, active from the middle Pliocene to date) and on a local scale (heterogeneously strained rock massif at the Antei uranium deposit). The development of a regional geodynamic model of geological structural units makes it possible to carry out procedures to ensure the safety of mining operations under complex geomechanical conditions that can expose the operating mines and mines under construction, by the Argun Mining and Chemical Production Association (PAO PPGKhO) on a common methodical and geoinformational platform, to the hazards of explosions, as well as to use the simulation results aimed at finding new orebodies to assess the flanks and deep levels of the ore field.

DOI: 10.1134/S1075701517030047

INTRODUCTION

The elaboration and application of models making a long-term forecast of the state of the geological medium and assessing the risk and consequences of the occurrence of extraordinary natural and technogenic events are currently among the key conditions guaranteeing the stable development of economic sectors where objects of elevated environmental hazard are functioning. The latter comprise mine fields, processing complexes, radiochemical enterprises, spots for isolating nuclear materials at various levels of radioactivity, dams, gas and oil pipelines, etc.

The complexity of creating long-term models is caused by the extensive themes of interdisciplinary problems being solved. Long-term forecasting is based on numerous geoscience disciplines, and each of them has its own object of study, methodical approach, means to obtain data, interpretation, representation, etc. The various scales (ranks) of the studied natural and technogenic processes play an important role in understanding these processes, which requires integrating the disconnected data characterized by spatial (global, regional, and local scales) and temporal (short-, medium-, and long-term forecasts) diversity.

Nevertheless, the scientific methodical basis has been generally formed to date, and the experience in creating and applying the long-term forecasting of the state of a geological medium has been gained, taking into account the geodynamic processes and seismic events that occur in it. The geodynamic grounds, which play the key role (*Kompleksnye ...,* 1984), are specially chosen territories (spots of rock massifs), where a complex of regular astronomic–geodetic, satellite, seismic, geophysical, geological, and other

observations are performed at points of a fixed network, and which are aimed at tracing deformations in the Earth's upper crust.

In the former Soviet Union, 60 geodynamic polygons were formed and functioned, with 34 of them focused on predicting earthquakes and estimating vertical motion rates in the Earth's crust; 12 of them were localized in areas adjacent to hydroelectric power plants with high dams; and 16 of them were in areas of petroleum mining. At present, new geodynamic grounds are being created in areas of intense technogenic activity. These are territories with large-scale mining works or underground constructions, e.g., the North Muya tunnel, Sakhalin oil pipeline, and the Eastern Siberia–Pacific Ocean pipeline system.

Depending on the aim of the geodynamic polygon, the measurements are performed during various time intervals: days, a few months, and a few years. The density of the measurement network is also controlled by the solved problems. The main condition, which is fulfilled in the course of designing the observation networks, is the outlet of the marginal data points into the background domains, relative to which the anomalous parameters of the studied object are measured. The observation points are spaced, as a rule, at a distance of 10–100 km from one another.

At the geodynamic grounds, the current horizontal and vertical displacements in various scales (ranks) and their parameters (direction, modulus, rate, focal earthquake mechanisms, etc.) are determined to reconstruct the present-day stress fields. The geodetic measurements, GPS control, seismological, and seismotectonic observations are used for this purpose, as well as to reconstruct the neotectonic stresses by the morphokinematic analysis of the fault's tectonics, numerical simulation of the geomechanical processes, etc. Using modern devices, in particular, laser deformometers, which ensure very precise measurements of the deformations in the Earth's crust and record large-scale seismic deformational wavy processes with unrestrictedly large periods (Dolgikh, 2000). Applying these instruments, the pulsatory stresses in the upper crust have been recorded in the Urals, the forerunners of earthquakes in the Baikal Rift Zone, and the conjugated wavy deformations in the Earth's crust. In addition, fractures and slickensides make possible to acquire tectonophysical estimates of the paleostresses (Sim, 1991). The seismological data on the mechanisms of earthquake sources give the characteristics of the current stress fields. The data on present-day stresses also allow us to select the active and hazardous faults from the general quantity of faults (Rebetsky et al, 2012; Rebetsky and Kuzikov, 2016).

The results of the research carried out on geodynamic grounds make it possible to regionalize the territory on the basis of the studied parameters and relationships between them, as well to localize anomalous (hazardous) sites. The trends of earthquake sources, large seismic events, including technogenic events, are determined in order to upgrade the techniques used to forecast them. In these studies, the modern methods of seismotectonics (*Paleoseismologiya,* 2011), as well as the techniques of interpreting plicative and disjunctive structural units based on the results of tectonophysical simulation (*Eksperimental'naya ...,* 1985), are used.

The current knowledge of the natural stressed state of the Earth's interior provides evidence of heterogeneous active stress fields and their variations under the effect of the existent geological processes. The interrelation between the stressed state and the topography in actively built up mountainous regions has been established. The stress values in massifs under their natural state show that the level of the stress deviator in the crust of intracontinental orogens does not exceed 500–700 bar, which is an order of magnitude higher than in the subduction zones of oceanic lithospheric plates (Rebetsky, 2015).

The hierarchical stress distribution in geological structures and their instability in value and direction are revealed even within separate blocks (Kuz'min and Zhukov, 2004). The instrumental studies in geodynamic grounds have revealed a complex spectrum of tectonic movements irregularly distributed in a discrete block medium. Trends and oscillatory displacements with various oscillation periods have been established. According to fundamental reasoning, rock massifs occur in the process of permanent deformation, and this should be taken into account when hazardous seismogeodynamic phenomena are forecast (Sashurin, 2002). The changeable geomechanical state of orebodies and host rocks revealed by Zhirov et al. (2016) may be related to the residual stresses acting in the rock massif due to the force of gravity.

At present, the views on the level and scale of the current geodynamic (seismic deformational) state of the Earth's interior are undergoing revision (Kuz'min, 2009). Understanding that recent geodynamics comprises deformation and seismic events proceeding in real time scale, many researchers emphasize the expanding role of the geodynamic factor in estimating the danger for territories with objects characterized by elevated technogenic and environmental loads (Kochkin and Petrov, 2015). It has been shown that in the case of the mathematical simulation of stresses, it is extremely important to take into account that a geological medium (primarily fault zones) may be in a supercritical state even before the application of an additional load (Rebetsky and Lermontova, 2014). This gives rise to a sharp increase in the far-ranging effect of loading and its dependence on the geodynamic regime of the stressed state (horizontal compression, extension, and shear).

The forecast of natural and technogenic hazardous phenomena is of special importance for objects using atomic energy (OUAE). In particular, these are enterprises for mining, concentrating, and processing ura-

nium ore (*Instrukziya* ..., 2000; *Federal'nye* ..., 2005). Among geological and geological engineering processes, phenomena, and factors of natural and technogenic origins, the seismotectonic faults, residual seismic deformations of the Earth's crust (seismic dislocations), recent differentiated motions of the Earth's crust, tectonic creep, and earthquakes of any genesis are subject to obligatory study and control in the areas where OUAE are located. In addition, monitoring the parameters inherent in processes and phenomena that are natural in origin, as well as periodically controlling the technogenic factors, must be ensured at all stages of the OUAE's life cycle.

In this respect, the results of elaborating the 3D deflected mode (DM) model of the geological structures of the Strel'tsovka uranium ore field (SUOF) in the southeastern Transbaikal region, as one of the key objects using atomic energy in Russia, are considered in this paper. Here, Argun Mining and Chemical Production Association (PAO PPGKhO) mines and processes molybdenum–uranium ore at deposits that are unique in terms of reserves. The study of contemporary seismic geodynamic processes is necessary to ensure the efficient planning and realization of undertakings for the rational management of the Earth's interior and environmental safety during the development of deposits of strategic mineral commodities under complex mining and geological conditions in the SUOF.

OBJECTIVES AND METHODS

The main objective of this study is to design a 3D model of the DM of rock massifs in the SUOF deduced from recent and older stresses, seismotectonic deformations of the surface with recognition and tectonophysical characterization of the active faults on the basis of the published geological and geophysical information and field study of the geological structural units.

To achieve this target, the following problems have been resolved:

—Designing a scheme of the fault's tectonics on a scale of 1 : 200000 with detailed spots on a scale of 1 : 500 based on the results of the geological–structural, mineralogical–petrographic, and structural–petrophysical mapping of the main fault zones in the studied territory;

—Elaborating a scheme of seismic dislocations on a scale of 1 : 200000 with detailed spots on a scale of 1 : 500 based on their mapping and structural–geomorphic data for the studied territory;

—Elaborating a scheme displaying the distribution of seismotectonic regimes (stress tensors) on a scale of 1 : 200000 based on the structural–kinematic analysis of the fault and fracture zones;

—Creating a 3D model of the DM of rock massifs deduced from a data complex on contemporary stresses and seismotectonic deformations of the surface with recognition of active faults and estimation of their seismotectonic potential.

Taking into account the specificity of the geological and tectonic structures of the studied territory, the works have been organized in three interrelated directions, each characterized by a certain set of methods: geostructural–tectonic, seismogeodynamics, and geodeformational. The results obtained were integrated on the common informational platform using technologies of 3D GIS: licensed ArcGIS 10, MapInfo Professional 10.5, and Global Mapper 11.

The geostructural–tectonic studies have been focused on certain features of faulting, localization of tectonically active faults, and recognition of the main stages of rearranging the stress field in lithospheric blocks for demarcating territory by geodynamic activity based on the GIS platform. The 3D models of the geological–tectonic structure of the lithospheric blocks have been worked out on the basis of a field study of the faults, the geodynamic setting, and the stressed state of rock massifs by tectonophysical methods at the reference deposits of the Strel'tsovka ore field (Antei, Argun, Tulukui, Strel'tsovka). The results of geostructural–tectonic studies became the basis of works in other directions.

The main aim of *seismogeodynamic studies* is to localize the generation areas of seismic phenomena at various depths in the 3D geological–tectonic model of lithospheric blocks. Based on this, the studies have been focused on the geodynamic processes and demarcation of the territory by the geodynamic settings, the elucidation of the geodynamic nature of seismically active lithospheric structures, and their role and place in the regional geodynamic evolution. The seismogeodynamic reconstructions covered a time span from the late Cenozoic to the present time. The conditions and manifestations of seismodislocations on the Earth's surface were determined using the interpretation of the remote sensing data, taking into consideration the Earth's surface topography, and studying the seismic activity of fault zones. The directions and rates of displacement of geoblock surfaces were determined by highly precise GPS geodetic methods.

The main objective of *geodeformational studies* is the tectonophysical simulation of the DM of rock massifs in the studied territory. For the calculations we used an UWAY program packet (Vlasov et al., 2004), which realizes the method of terminal elements. The simulation results were verified at the regional and local levels. At the regional level, the fault zones with extension, compression, and shear deformations revealed in the process of simulation were studied in detail, including the driving of trenches and sinking of dug holes. The Klichka Fault, which has been active from the middle Pliocene to the present time (~ 5 Ma), including the tracks of a strong earthquake, as the seis-

mic dislocations dated back to the early Holocene (Chipizubov et al., 2013), is one of these structural units. At the local level, the simulation results have been verified by the data of the long-standing deformational and seismoacoustic monitoring of the highly stressed rock massif at the operating Antei uranium deposit (Rasskazov et al., 2012, 2014).

RESULTS

The Argun Lithotectonic Zone, or the Argun Tectonic Block, as an area of the widespread Late Mesozoic magmatic activity, is a part of the Mongolia–Argun volcanic belt in the southeastern Transbaikal region (*Geologicheskoe ...,* 1997). This block is characterized by the early consolidation of the basement (Andreeva et al., 1996; Rybalov, 2002) and by the development of large volcanogenic structural units (Kuitun, Strel'tsovka, Kuladzha), which make up a chain in its southern framework (Vol'fson et al., 1967; Solov'ev et al., 1977; Ishchukova et al., 2007).

The geology of the Argun Lithotectonic Zone as a whole and of its particular tectonic elements (Fig. 1) shows that they are largely composed of the pre-Mesozoic orogenic rocks with inclusions of volcanic–plutonic complexes up to Mesozoic in age. These rock complexes probably correlate with the Paleozoic (Caledonian and Variscan) structural units, which are exposed to the southeast within the Greater Khingan in the territory of China. The Argun Zone is separated from the Archean–Proterozoic and Paleozoic granitoid complexes of the Stanovoi Domain by the deep Mongolia–Okhotsk Suture, and by its eastern Aga River branch from the terrigenous rocks of the Aga River Zone.

The observed distribution of granitoid and volcanic–sedimentary complexes shows that in the Mesozoic the regional structures were formed in the extension setting (rifting). In the post-Mesozoic time, this territory developed in the platform regime, along with the short-term activation of tectonic processes related to the evolution of the Baikal Rift Zone.

The maps of the topography and gravity anomalies show that the regions of relatively elevated tectonic intensity may be conventionally divided into localized and extended, e.g., along the Argun River and to the northeast of the Dauria Settlement. The areas with reduced tectonic intensity are related to the extended basins striking in the NE–SW direction, which give evidence of linear tectonic blocks bounded by the NE–SW-trending faults dominating in the block structure of this territory. The detailed gravimetric data show that the negative gravity anomalies (–50 mGal) related to the basins are combined with positive anomalies (40 mGal) at uplifts. Thus, the positive gravity field correlates with the topographic uplifts composed of granitoids differing in age. It may be suggested that the formation of gravity anomalies is primarily determined by topography rather than by a specific regional deep structure.

Recent Horizontal Movements of the Surface and the DM of Rocks

The measurements of the rate and orientation of the recent horizontal movements near the SUOF performed for the first time with the GPS geodetic method have shown that the geodetic observation points located at the walls of the Sukhoi Urulyungui Basin are shifted in the ESE direction (Fig. 2). It has been established that rate of horizontal movements vary from 20 to 25 mm/yr. Judging by the large ellipse of errors, the measurements at the observation points were carried not out with sufficient accuracy. An additional series of measurements are necessary to ensure sufficient accuracy under the conditions of minor deformations typical within plate domains.

The horizontal deformations based on the results of GPS observations were calculated using triangulation, that is, calculation of the changed lengths of the sides of four triangles, at the vertices of which the GPS observation points are located, has shown that horizontal elongation for three triangles took place to the NW (two triangles) and to the NNE (one triangle), along with a minor horizontal shortening toward the NE and the ESE, respectively (Fig. 2). If we assume that tectonic deformations do not result in a change of volume, then the maximal shortening for these triangles develops in the vertical direction. Thus, we are dealing here with a geodynamic type of the stressed state corresponding to horizontal extension. Another triangle of the calculated deformations yielded the maximal shortening in the northwestern direction, along with a very small northeastward elongation in contrast to the other three triangles. Using the above suggestion for the fourth triangle, we find that the maximal elongation is oriented in the vertical direction. This corresponds to the geodynamic regime of horizontal shortening.

Such a substantial difference in the regimes of stressed states for the adjacent crustal blocks is explained by the results of the tectonophysical reconstructions of the present-day stressed state of intracontinental orogens of the Altai–Sayan and the Northern Tien Shan. Rebetsky et al. (2012) has shown that in the areas of uplifted ridges, the setting of horizontal compression or shearing (transpression) is predominant, whereas the setting of a horizontal extension or shearing (transtension) is predominant in troughs and lowlands.

It should be noted that GPS observation points are localized on mountain ridges. The areas where rates of surface displacements have been estimated comprise mountain uplifts and basins dissected by tectonic faults. Only triangle of the KRNS–KRNK–KRNE stations reflects the present-day displacements by sta-

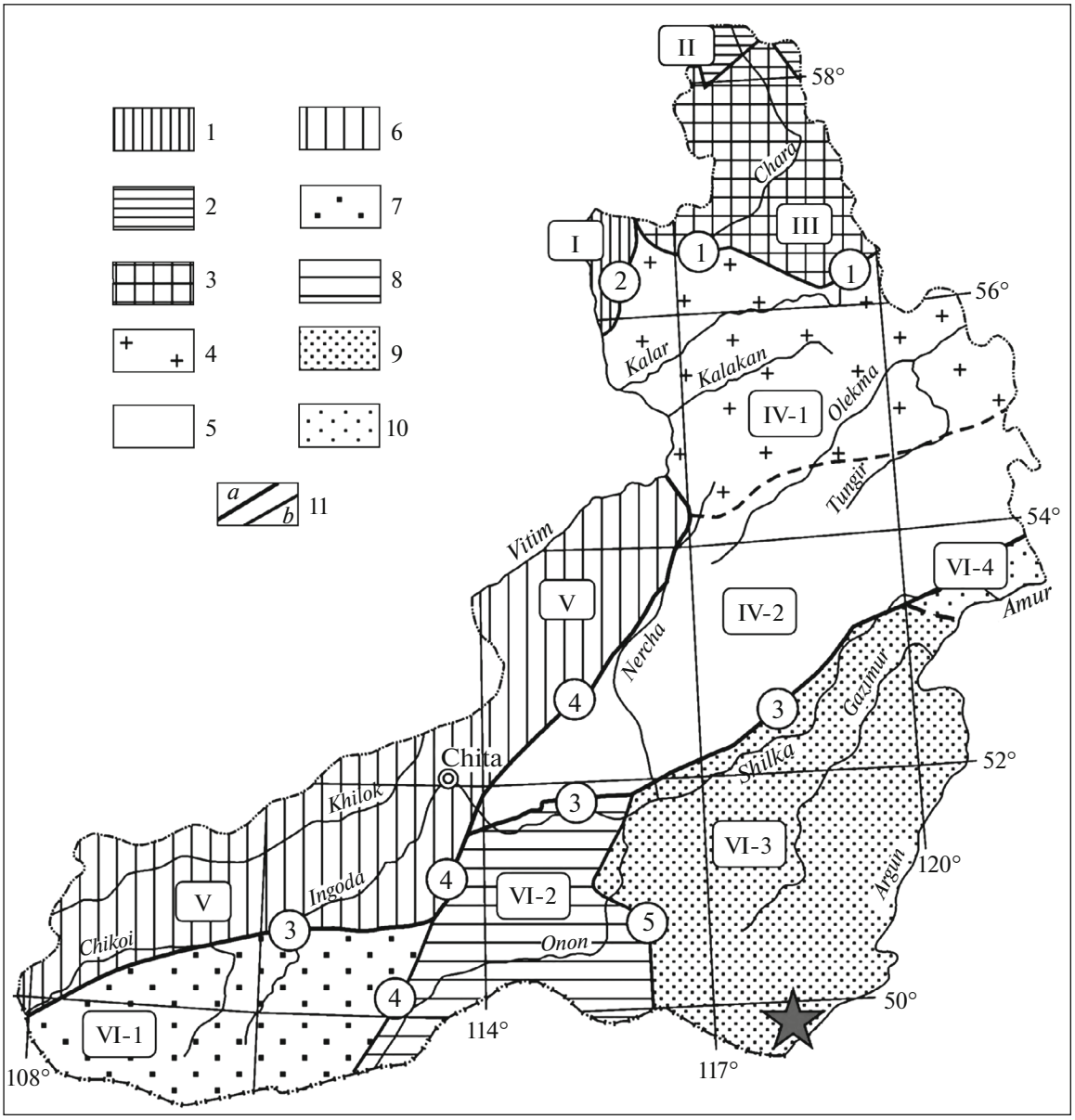

Fig. 1. Tectonic regionalization of Transbaikal region (Geologicheskoe ..., 1997). (1) Baikal–Vitim System; (2) Siberian Platform; (3) Aldan Shield; (4) Stanovoi Region; (5) West Stanovoi Domain; (6) Selenga–Yablonovy Region; (7) Hentiy–Daur Zone; (8) Aga River Zone; (9) Argun River Zone; (10) Upper Amur River Zone; (11) structural boundaries: (*a*) master faults bounding fold regions, (*b*) faults of second order bounding lithotectonic zones (dash lines are inferred zones). Numerals in boxes: (I) Muya Zone, (II) Berezovsky Zone of plate cover, (III) Kodar–Udokan Zone, (IV-1) Kalar Zone, (IV-2) West Stanovoi Domain, (V) Khilok–Vitim Zone; (VI-1) Hentiy–Daur Zone, (VI-2) Aga River Zone, (VI-3) Argun River Zone, (VI-4) Upper Amur Rver Zone; faults (numerals in circles): (1) Stanovoi; (2) Vitim–Nercha; (3) Mongolia–Okhotsk, (4) Ongon–Tura, (5) East Aga. Area of study is marked by star.

tions, which are localized within one mountain edifice, when the basic lines do not intersect the basins. A regime of horizontal shortening has been obtained only fo this block, which includes the Strel'tsovka ore field. The data on the rates of the current horizontal movements and orientation of deformation axes corresponding to shortening and elongation near the town of Krasnokamensk are used by us to form the calculation model of the present-day DM for rock massifs in the Strel'tsovka ore field.

The studied region is characterized by weak seismicity (*Komplekt ...,* 1999). Therefore, to estimate the present-day DM of rock massifs from the data on mechanisms of earthquake sources, a vast territory with coordinates 44°–54° N and 110°–124° E is considered. As follows from various published sources, the solutions of focal mechanisms for 17 events are known for this territory as a whole; four of them have been obtained by various methods. Stereograms of the focal mechanisms and their classification diagrams show

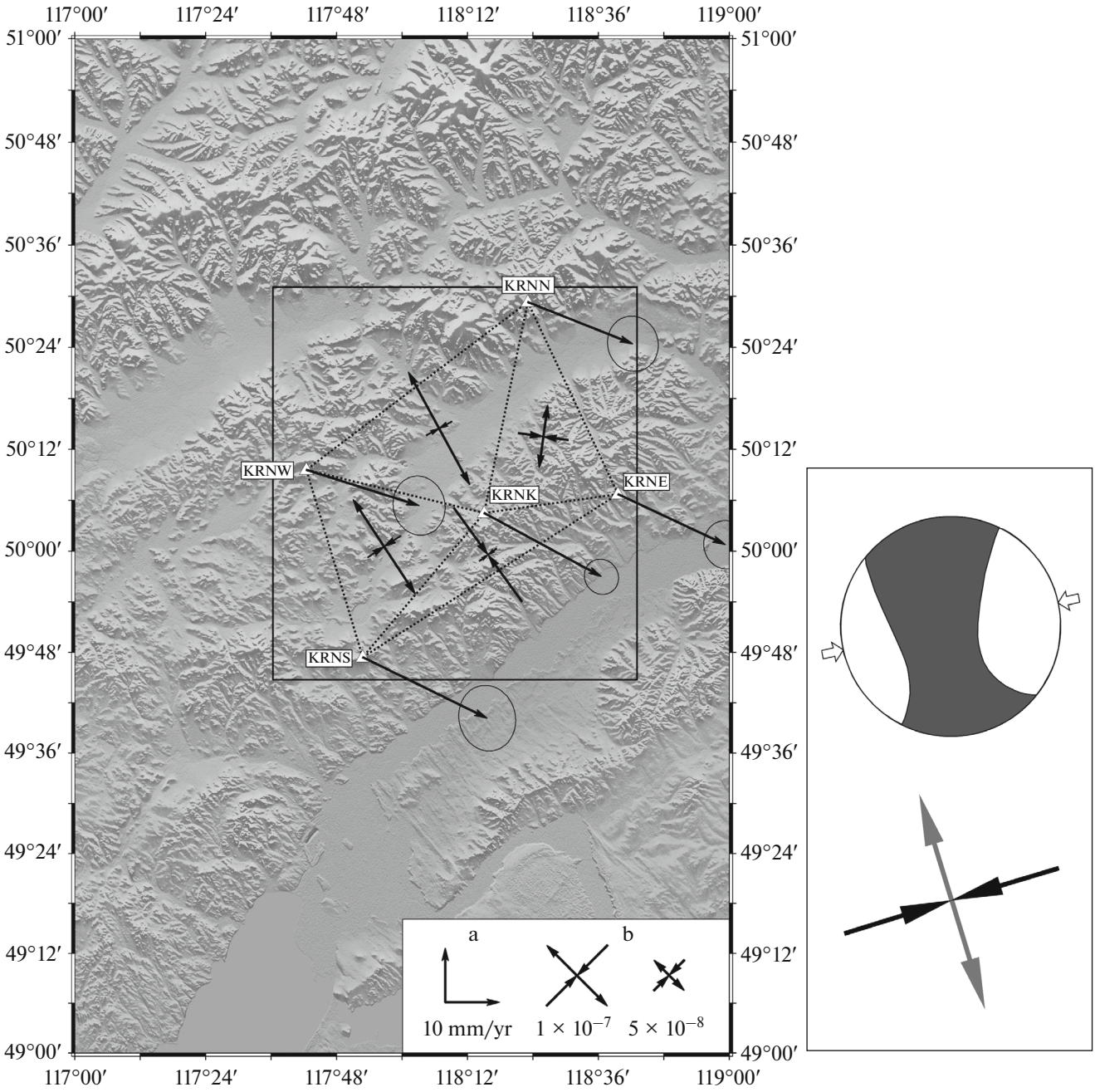

Fig. 2. Present-day DM of deformation in southeastern Transbaikal region. On left: rates of present-day horizontal movements and relative deformation of geodetic network in area of Strel'tsovka ore field: (a) vectors of movement rate, mm/yr of GPS points (KRNK, KRNW, KRNN, KRNE, KRNS) from results of measurements in 2011–2013, International Terrestrial Reference Frame (ITRF2008), confidence interval is 95%; (b) rates of principal horizontal deformations, 10^{-1} mm/yr. Convergent and divergent arrows are axes of shortening and elongation, respectively. Square denotes ground of observation and tectonophysical simulation (see text for explanation). On right: mean mechanism of earthquake (above) and orientation (below) of principal compression (convergent arrows) and extension (divergent arrows) in district.

that the majority of earthquakes are characterized by the shear type of displacements in the source; a few reverse-type events and two earthquakes of the normal-fault type are recorded. The available data on earthquake source mechanisms allow us to determine the average mechanism and orientation of the principal compressive and tensile stresses, using the method proposed by Yunga (1990). The obtained results show that the average mechanism is close to the shear type. The compression and extension axes are nearly horizontal: the compression axis is nearly latitudinal and the extension axis is nearly meridional (Fig. 2).

Using the results of observations to clarify the geodynamic settings in the southeastern Transbaikal region, we note the conclusion obtained for the Baikal geodynamic ground with the GPS network comprising up to 20 stations (San'kov et al., 1999, 2005; Lukhnev et al., 2010). This conclusion does not rule out the effect of the internal lithospheric source—ascent and spreading of anomalous mantle matter—on horizontal movements in the Baikal Rift, although the calculations by Lesne et al. (1998) have shown that present-day deformations can be explained only by horizontal forces related to the remote sources at the plate boundaries. Thus, the separate consideration of the current deformations even within the context of a more extensive polygon does not allow us to answer the question on the causes of the observed deformations and connect them with the block transfer induced by the remote sources, which may be regarded as the boundaries of the tectonic plates.

As also follows from San'kov et al. (1999), in the case of numerical simulation based on the equivalent model medium, the necessity arises to determine the loading model, which includes internal and external loads. The loads are set in the displacements, pressure, and forces at the boundaries of the tectonic blocks, as well as the internal loads, which are caused by the density heterogeneities, influence of temperature effects on geological materials, and distribution of stresses, taking into account the rheological features of the rocks, as a reaction to an external impact. Erosion and sedimentation, the temperature field (e.g., related to volcanic activity), fluid dynamics, and other phenomena play an important role in formation of the contemporary structures (Sherman, 2009).

In a natural medium, the existing DM of rocks and geodynamic phenomena are formed due to the gradual and simultaneous influence of all the aforementioned loads against the background of the evolution of the structure and properties of the rock complexes during the history of the formation of the observed contemporary structure. The division of the effects of external and internal loads in the course of simulation is an accepted abstraction necessary for the numerical computation and is caused by the completeness of modern knowledge on the geological, geophysical, and geodynamic features of the considered object. This emphasizes the importance of the preliminary consideration of the regional geophysical features, geodynamics, and tectonics.

The presented data allow us to conclude that faults and rock complexes making up the NE–SW-trending uplifts and basins are the main structural elements of the territory. These structural elements are well expressed in the geological pattern, topography, and magnetic and gravity anomalies.

The following episodes in the formation of the contemporary geotectonic structure are recognized in the publications on fault tectonics and the DM of rocks in the area close to the SUOF (Petrov, 2007; Petrov et al., 2010):

—During the period of preore (pre-Mesozoic) preparation, the regime of domal uplifting with an additional near-meridional compression component was predominant;

—Inversion of tectonic stresses induced by the rearrangement of the global tectonic stress field in the Late Triassic–Middle Jurassic (Delvaux et al., 1995, 1997). At this stage of tectogenesis, the orientation of the horizontal compression axis changes from near-meridional to near-latitudinal. Along the East Urulyungui and South Argun transblock fault zones, the right-lateral normal–strike-slip offsets are realized with the concomitant development of the transform valley, where the near-parallel fault systems constrain the tectonic blocks in a pull-apart-type structure;

—In the Late Jurassic–Early Cretaceous, the local pre-caldera dome was formed; the near-latitudinal chain of volcanoes (Aerodrom, Krasny Kamen, Maly Tulukui) developed in its axial part. Their eruptions resulted in the exhaustion of the magma chamber, sagging of the surface, formation of the caldera, and filling of the caldera with sedimentary and volcanic materials. The compensatory Sukhoi Urulyungui Basin was formed beyond the caldera. After collapse of the caldera, the vein, stockwork, and stratal orebodies were formed in the SUOF.

Thus, the system of NE–SW faults in the framework of regional faults may be regarded as the basic one. In combination with the near-latitudinal and near-meridional faults, this system of faults was formed at the very early stage of tectogenesis and emplacement of granitoid rocks. The vertical movements expressed in the local volcanic activity, along with the formation of the Strel'tsovka and Kuitun calderas gave rise to the development of isostatically compensating geological structures, e.g., the Sukhoi Urulyungui Basin.

The results of the structural, morphostructural, and geological studies suggest that no significant vertical block movements took place at the neotectonic stage; however, the question on the structure of the neotectonic stress field remains open. According to the method proposed by Sim (2011), the statistically most numerous solutions for the Late Cenozoic indicate a northwestern extension and a northeastern compression. As follows from the mechanisms of earthquake sources, the present-day stressed state is characterized by an NNW–SSE extension and an ENE–WSW compression. The preliminary GPS measurements show an NNE–SSW elongation and a WNW–ESE shortening in the Sukhoi Urulyungui Basin. If it is accepted that the Holocene Klichka seismic dislocation was a reverse fault with strike-slip components, then the mean compression in the Late Cenozoic may have varied from near-meridional to northeastern—the latter is the most probable.

Tectonophysical Simulation of Stresses in the Earth's Crust

There are two main approaches in the study of the stressed state in rock massifs:

—Based on the natural stresses studied with field tectonophysical methods (Gzovsky, 1975; Gintov, 2005);

—Based on the equivalent model medium studied with physical (Mikhailova, 1989; Osokina, 1963; Bornyakov, 1980) or numerical (Stefanov, 2008) simulation.

The methods of field tectonophysics are, as a rule, applied to solve an inverse problem, i.e., restoration of the formation history of the present-day stress field from the fracture systems of various ranks, in combination with a structural study. As a result, a geological model of the present-day geotectonic structure formation is created, and the genesis of the contemporary stress field is explained on its basis. The reviews of these methods are published by Rebetsky (2002), Sim (2011, 2013), and Nikonov (2011).

The tectonophysical methods, which suggest numerical calculation with the application of modern computing complexes, are focused on the solution of the direct problem: the determination of the DM of rocks based on the available equivalent model of the geological medium and its tectonophysical interpretation (Pogorelov et al., 2010; Voitenko et al., 2013). The study of the rheological properties of rocks and the qualitative simulation of the characteristic phenomena, e.g., faulting in the lithosphere, are connected with laboratory modeling based on rock samples and with the use of the equivalent materials (Bornyakov, 2012).

The numerical simulation assumes the following three stages:

—Construction of the equivalent numerical model of the medium;

—Calculation and correction of the initial model;

—Interpretation of the results obtained (features of the calculated DM) jointly with the geological–geophysical data on the geological object and the results of determining the stress and deformation fields using other methods, e.g., field tectonophysics.

We will follow this sequence in the subsequent text.

At the first stage, we propose creating two preliminary models:

—The model of the structure and properties is created on the basis of the geological-geophysical data. The determinant relationships and rheological links are accepted. It is suggested that the model must adequately reflect the gravitational stressed state.

—The model of boundary conditions is constructed on the basis of the regional geodynamics, seismic regime, and character of present-day movements, as follows from the cosmic geodesy and remote sensing. The boundary conditions (evolution of boundary conditions) are determined. They make up the contribution of the tectonic and supplementary exogenic (technogenic) loads. It should be noted that it is not a simple task to estimate the contribution of the tectonic stresses and especially their evolution during the formation of the geotectonic structure.

At the second stage, the numerical calculations are being performed. The stressed state obtained is verified for coincidence with the data on natural stresses, e.g., using the method of cataclastic analysis (MCA) in the case of sufficient data on the regional seismicity or the modification of the MCA based on determinations from shear fractures (Rebetsky, 2011). Additional data on the geological and tectonic features of the structure under consideration are also involved. The correctness of the created model is estimated.

At the third stage, the preferable simulation variants are comprehensively compared. The geological, geophysical, geotectonic, and geodynamic senses of these variants are established.

Note that studying the deformation mechanisms of natural objects based on the set of geological, geophysical, or tectonophysical data resolves an inverse problem of geodynamics, including the force source of loading in the local area of the Earth's crust. This requires enumerating the possibilities for numerous solutions of direct geomechanical problems. For a narrow set of parameters, combined with the complexity of comparing the simulation results and the real natural object, the uniqueness of the solution is not achieved (Rebetsky, 2015). It can be attained by including additional comparison parameters , e.g., the data on the present-day and older stresses (orientation of the principal stress axes), as well as on gravity anomalies.

Note that the validity of the chosen strength parameters determining the solution plays an important role in geomechanical simulation. The results of the laboratory experiments on the failure of rocks and the results of the tectonophysical studies of stresses (Rebetsky, 2011, 2015; Rebetsky and Kuzikov, 2016) are helpful in this respect. The loss of strength under fluid pressure in fractures and porous space according to Darcy's law is also extremely important for the calculations. To a first approximation, fluid pressure may be taken into account by the reduced coefficient of internal friction (Pogorelov et al., 2010).

Tectonic Structure of Territory as the Basis for the Equivalent Numerical Model

The conceptual 2D and 3D models of the territory have been created on the basis of a generalized schematic map of the geological complexes and the main faults (Fig. 3).

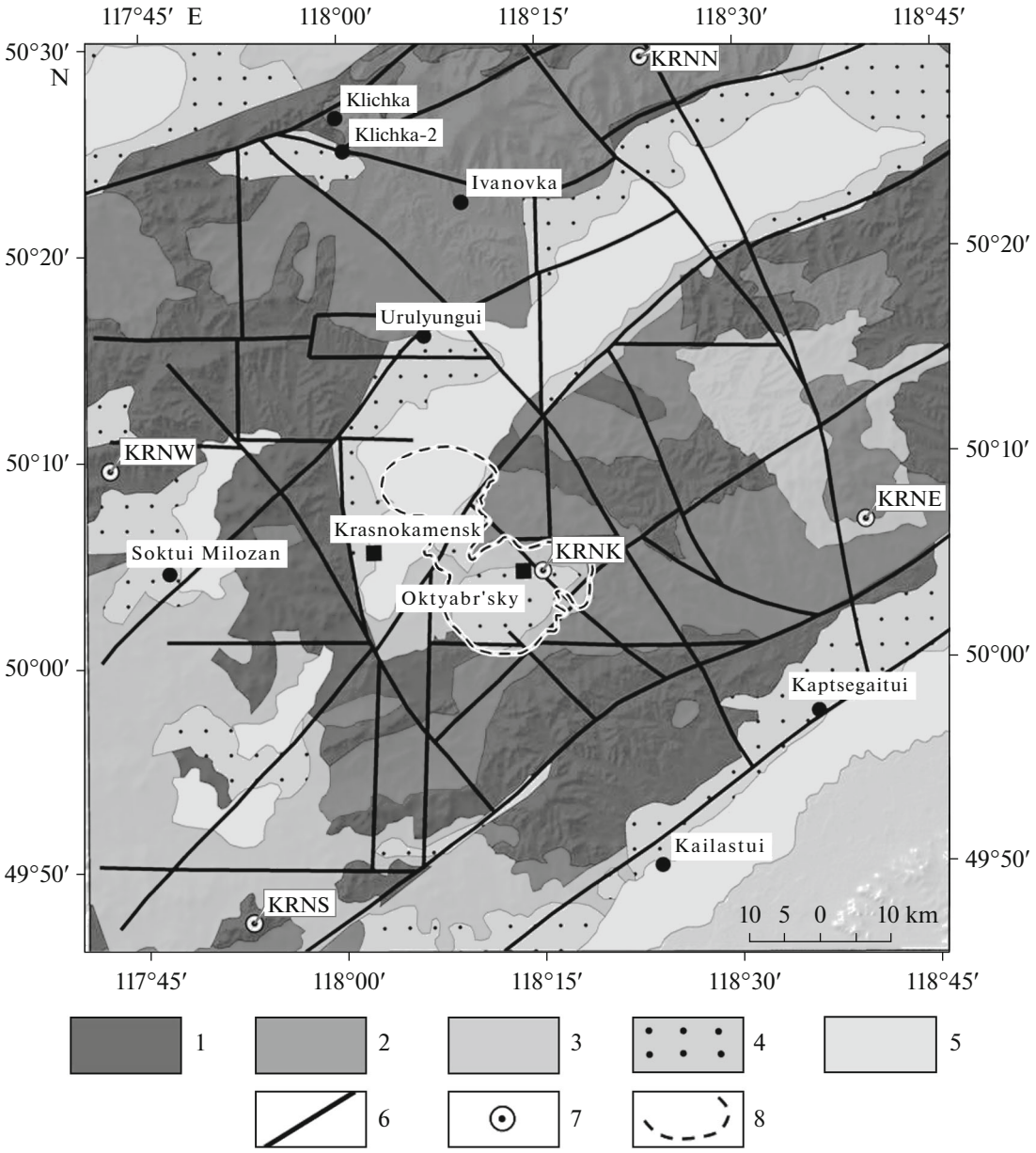

Fig. 3. Geological rock complexes and faults in Strel'tsovka ore field. (1) Archean and Paleoproterozoic granite gneisses and migmatites; (2) Middle Paleozoic–Mesozoic granites; (3) Mesozoic volcanic–sedimentary complexes; (4) Cenozoic sedimentary–volcanic complexes; (5) Neogene–Quaternary sediments; (6) main fault zones; (7) GPS geodetic points; (8) contour of Strel'tsovka uranium-bearing caldera.

Taking into account the transverse dimensions of the simulated region, the following assumptions have been made:

—Because of the thinness of various sedimentary rocks, the latter are not differentiated by their genesis;

—Because of the slight differentiation of the geomechanical properties of pre-Mesozoic granite gneisses and granitic intrusive rocks, their particular properties are replaced with the mean values;

—Topography is schematized and reflects only the most significant morphostructural features of the surface;

—Lineaments have been replaced with a fault body (Romanyuk et al., 2013; Voitenko et al., 2013). In the spots of adjoined and intersected faults, their position on the surface has been corrected to avoid terminal elements of "bad" geometry (minor angles between neighboring elements) of the numerical model;

—It is suggested that a fault body is translated over the entire simulated depth (down to 10 km). The offsets along the faults are controlled by the horizontal tectonic movements and by the variation of the lithostatic pressure with depth.

The first three assumptions are made in order to avoid thin structural domains, which would lead to terminal elements with side proportions less than 1 : 5; the latter are unfavorable for the calculations.

The aforementioned features do not lead to a restriction of the general results obtained for geostructures with the accepted geometry of the faults.

The structure of the fault body is accepted to be similar to that in Chester et al. (2005) and that discussed by Romanyuk et al. (2013). Despite the zone of the main fault plane, localizing the tectonic slip, has a characteristic width of 0.5–2.0 m, the fault is placed in a core consisting of rocks which have undergone intense deformation and destruction. This region is characterized by lowered seismic velocities and elevated absorption of seismic pulses, lowered electric resistance, and elevated porosity (Ben-Zion, 1998; Ben-Zion and Sammis, 2003). These data closely correlate with the results of studies of active faults (Kuz'min and Zhukov, 2004) and with the physical simulation of faulting in equivalent materials (Seminsky et al., 2013). The fault body is characteristic in width (a few hundred meters). The strike-slip offsets along the faults are primarily related to the occurrence of "weak" minerals in the fault body, elevated fluid saturation, etc. In our case, the lineaments are considered only as the structural elements necessary for a relative offset of the tectonic blocks. The stresses within the fault zones are not incorporated in the summary stress field.

The results of tectonic stress field analysis based on the morphostructural method (Sim, 2011, 2013) were also used as the initial data for the numerical simulation. The orientation of the compression and extension axes as a projection on the horizontal plane was obtained in the course of reconstructing the stressed state along the lineaments. The orthogonal compression axes indicate a triaxial stressed state of the rocks (Fig. 4).

The localization of the normal faults shows that situations when dipping limbs adjoin the basins from opposite sides are very rare. Therefore, it may be proposed that the intermontane basins were primarily formed in the process of the vertical displacements of the underlying structural layer. Such a setting could have been realized due to a vertical uplift of the mountainous massifs with the formation of normal faults followed by the subsequent sinking of the intermontane basins and their filling with sediments. If the aforementioned displacements were controlled by the ascent of magmatic material, they would be characterized by lower gradients within the Argun Lithotectonic Zone and by a lack of strikingly expressed normal faults around the mountain massifs. Undoubtedly, additional geological and geophysical data are needed to substantiate this conjecture. In our studies, this hypothesis has been verified by numerical 3D simulation.

As can be seen from Fig. 4, the left-lateral strike-slip offsets dominate in the NE–SW-trending faults. Such a setting is evidence of the leading role of single-axis compression in the NNE–SSW direction. The orientations of the projections of the main stress axes are shown in the network of faults selected for numerical simulation.

Based on a complex of geophysical data, including electric sounding and a radon survey, the possibility of a near-vertical attitude down to a depth of 10 km has been shown for the fault zones (fault bodies) (Seminsky et al., 2013). This model is consistent with the geological assumption that faults in the Argun Tectonic Block extend to a depth. This assumption is supported by the geophysical data (Dukhovsky et al., 1998). In constructing a numerical model of the geostructure, we assumed steeply dipping (vertical, without loss of generality) interblock fault bodies extending down to 10 km, although certain structural elements, e.g., the Klichka Fault, could have been reverse strike-slip faults.

Structure and Properties of the Medium Assigned to Simulation of Tectonic Stresses

The petrophysical properties of rocks are chosen to be characteristic of the phase composition established on the basis of the experimental data for rock samples and rheological parameters used for calculating gravitational stresses at the upper levels of the Earth's crust in the region that hosts deposits of the Strel'tsovka ore field (Petrov et al., 2014, 2015).

The computed 3D model consists of more than 40000 elements, the sides of which are primarily triangular or quadrangular. The characteristic size of the elements in the model is 2 km.

The areas of the faults are determined as 400 m wide in the plan view. The nodes of the model were created first in the areas of the granitoid massif (basement), and then a network was generated from them. The 3D model consists of three layers fundamentally important for simulation:

—The heights of 1000–0 masl conventionally comprise generalized topography and near-surface heterogeneities according to the structural pattern of the territory. The heights are simulated by the Drucker–Prager plastic body taking into account the effect of compacting pressure on failure;

—The depths of 0–10000 m are a granitoid framework with a faulting structure. The faults extend vertically throughout the above-mentioned depth interval. The detailed data on their dip angles are unknown.

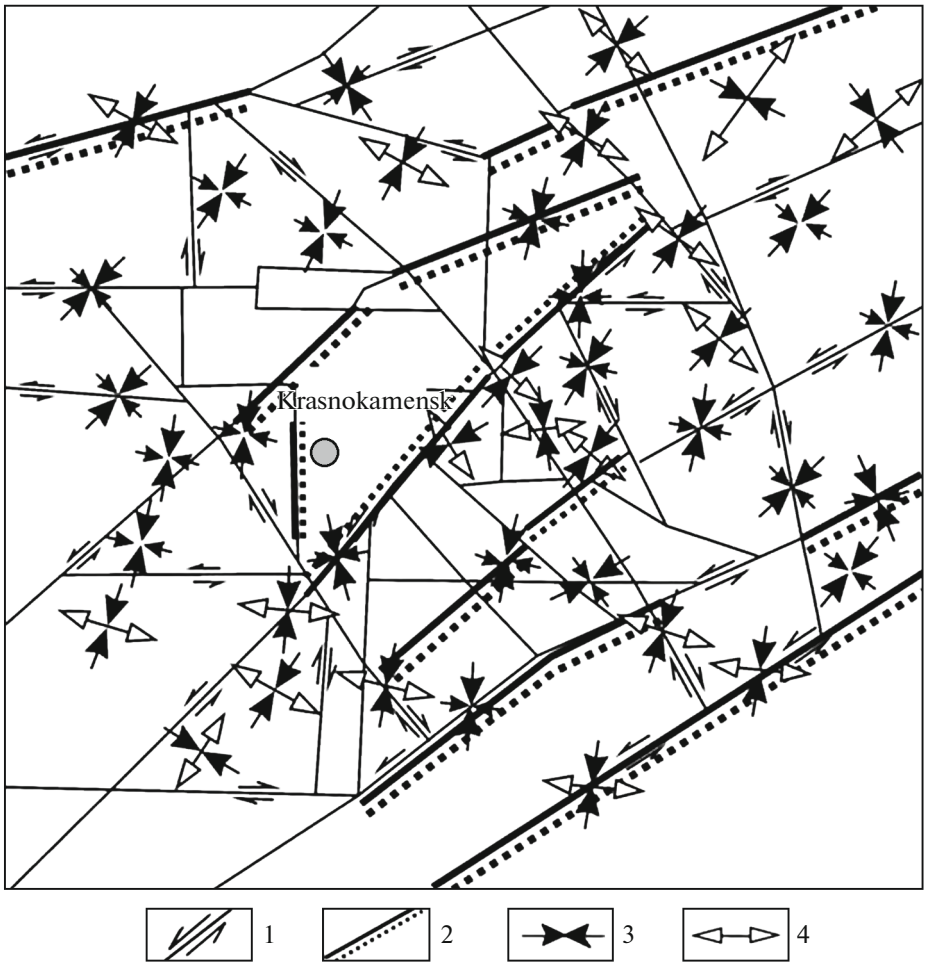

Fig. 4. Faults with orientation of principal stresses and kinematics of fault zones at neotectonic stage of tectogenesis restored with morphostructural method (Sim, 2011). Fault network has been created from geological data on scale of 1 : 200000–1 : 50000, results of interpretation of topographic maps and cosmic photographs, after Petrov et al. (2010) with supplements. (1) Main faults and direction of displacement of their walls; (2) largest normal faults; lower wall is marked by dotted line; (3) compression axis; (4) extension axis.

The structural domains are simulated by the Drucker–Prager plastic body.

—The depths of 10000–15000 m are the underlying structural domain (region 4 in Fig. 5, Table 1), which was introduced in the model for setting additional vertical loads (in transfers). Plasticity according to Mizes is realized here (plastic deformations develop if the arising tangent stresses exceed the plasticity limit; the coefficient of internal friction = 0).

The plan of the main fault zone framework in the area of the SUOF is represented in Fig. 6. The calculated network in the 3D realization is given in Fig. 7.

Choice of Loading Model and Results of 2D Simulation

To estimate the contribution of tectonic stresses and especially their evolution during the formation of a geotectonic structure is usually not a simple task. Let us consider a mode of appraisal of external (additional) tectonic stresses in the absence of obvious evidence of the geodynamics of the simulated region. For this purpose, we will take a flat 2D model cutting across the geostructure in the plan view; then we will preliminarily estimate the effect of certain boundary conditions, which may be compared with the probable tectonodynamic settings in the studied area. The suppositions for the formation of boundary conditions are based on the behavior (rheology) of the rock samples deduced from the experimental data, on the tectonic movements, and the possible deformation impacts in the area close to the SUOF.

Note that the area of the stressed state is distant from the outer boundaries of the presented fault system (Figs. 3, 4). Thus, we do not expect the correct amplitudes of the horizontal displacements at the boundaries to distort the results in the analyzed area. A certain lateral resistance will also be brought about in the absence of the boundary conditions of fastening

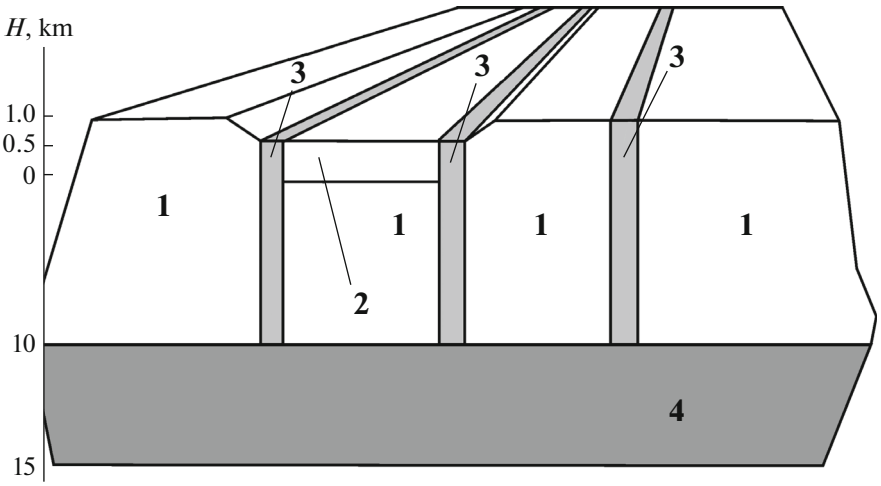

Fig. 5. Schematic vertical section reflecting structure of simulated geotectonic structure. See Table 1 for properties of model layers.

at the vertical boundaries, which realizes the extension of the blocks bounded by the NE–SW-trending faults in the direction to infinity along the strike.

We consider models of marginal conditions and calculations for vertical clamping, which coincide with the north–south direction with respect to a sheet of paper, combined with additional lateral support and a left-lateral strike-slip fault. The results of the calculations are reflected in the following graphics:

—Loading scheme. The horizontal constituent is equal to half of the vertical component. Amplitude of the vertical displacement is 250 m;

—Displacement amplitude, m. Direction of surface displacement is denoted by the short dashes; the heavy zigzag dashes are the displacement paths;

—Tectonic pressure, MPa;

—Maximal tangent stress, MPa;

—Lode-Nadai coefficient, or 3D deformation (in some cases);

—Projections of principal stress axes (algebraic maximal and minimal) on the horizontal plane juxtaposed with the fault network, orientation of the principal stresses, and kinematics of the fault zones at the neotectonic stage established by the morphostructural method.

The linear dimensions in km are denoted along the vertical and horizontal axes of the graphic images. The location of the Argun River coincides with the NE–SW-trending lineament bounding the North Khingan Tectonic Block (TB), see Fig. 6.

Table 1. Properties of materials accepted in numerical model of fault–block structure in area of Strel'tsovka ore field

No.	Geological associations	Density, g cm^{-3}	Young's modulus, GPa	Poisson's ratio, non-dimensional	* Angle of internal friction φ_{DP}, degree	Limit of plasticity (cataclastic flow), GPa
1	AR–PR–PZ_1 granite gneiss and complexes of igneous rocks, PZ(MZ) granitoid intrusions	2.55	80	0.20	2.9	0.09
2	MZ (J_3-K_1) volcanic–sedimentary complexes, K_1 and N–Q sediments	2.45	40	0.30	7.4	0.04
3	Fault zones	2.40	10	0.35	17.5	0.01
4	Granite gneiss, granitoids and metamorphic rocks of structural domain at depth of 10–15 km	2.65	120	0.25	0	0.015

* Angle of internal friction φ_{DP} related to angle of internal friction at brittle failure φ_C and to traction coefficient, after Coulomb by relationship k: $\alpha = \tan(\varphi_{DP}) = \frac{2\sin(\varphi_C)}{\sqrt{3}(3-\sin(\varphi_C))}$, $k = \frac{6c\cos(\varphi_C)}{\sqrt{3}(3-\sin(\varphi_C))}$.

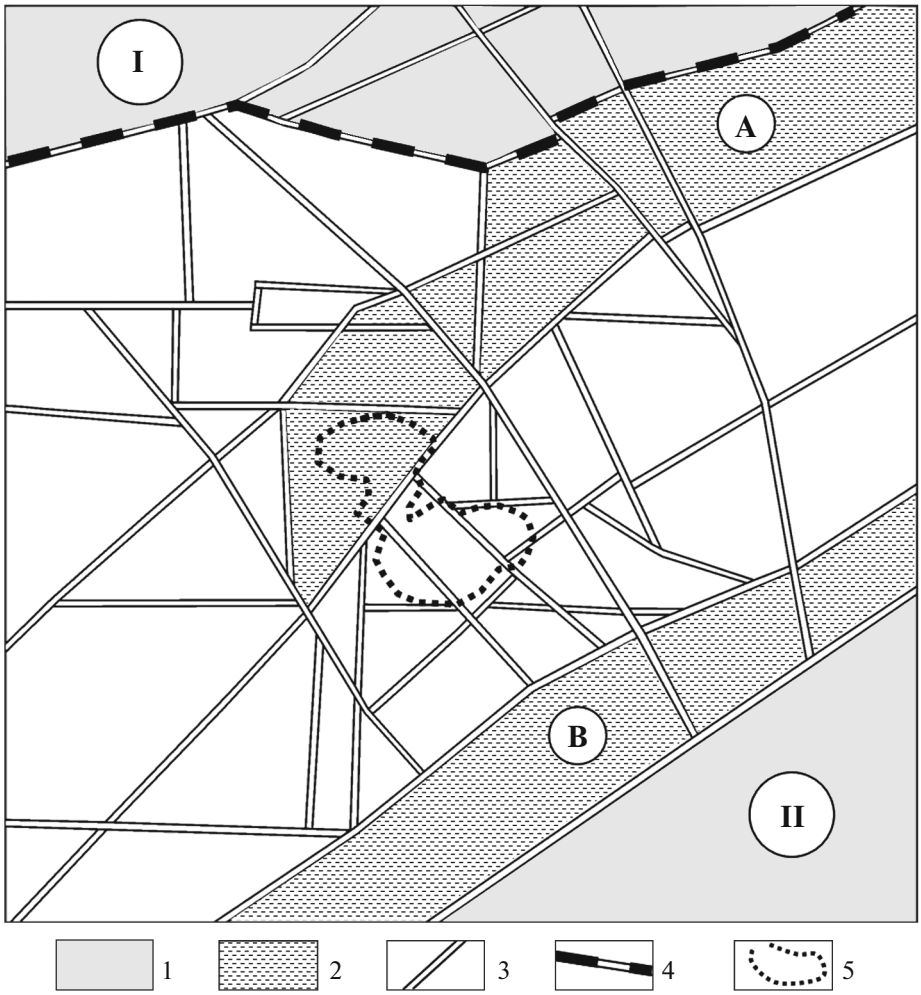

Fig. 6. Plan of fault structure as basis of calculated model assigned for study of tectonic stress field. Framework of faults is presented in Figs. 3 and 4. (1) tectonic blocks: I, Gazimur–Klichka; II, North Khingan; (2) intermontane basins: A, Sukhoi Urulyungui; B, South Argun (Argun River valley); (3) main interblock fault; (4) Klichka Fault (seismodislocation); (5) contour of Strel'tsovka caldera.

The tectonic features of the SUOF region, which are taken into consideration by the choice of the boundary conditions, are as follows:

—North Khingan TB (the block in the southeastern corner of the model) ensures the setting of the left-lateral strike-slip faulting;

—Gazimur–Klichka TB (the block in the northwestern corner of the model also ensures setting the left-lateral strike-slip faulting);

—The system of NW–SE-trending faults is younger than the NE–SW-trending faults, and the latitudinal and meridional faults;

—The NE–SW-trending faults make up the main fault system, within which the general setting of the left-lateral strike-slip faulting is observed;

—Setting the horizontal extension is inherent in the Sukhoi Urulyungui Basin close to the Dosatui Settlement, see Fig. 4.

We consider some characteristic results of the DM calculation for rock massifs, taking into account the kinematic features of the fault zones in the studied territory. The rock properties in the fault zones (Table 1) are matched in such a way that not only could the effect of the plastic flow be realized but that also allowed analyzing the obtained pattern in terms of revealing the style of loading that gave rise to the occurence of the observed deformations verified under field conditions. All the calculations were carried out under dynamic conditions; i.e., the model underwent loading with a gradually increasing amplitude.

The calculation results displayed good continuity in the variation of the DM. Because of the absence of of well-expressed structural boundaries beyond loaded tectonic blocks, other boundaries were not fastened. It was assumed that such marginal conditions ensure the inheritance of the revealed lineation of the tectonic blocks in the NE–SW direction. It was also

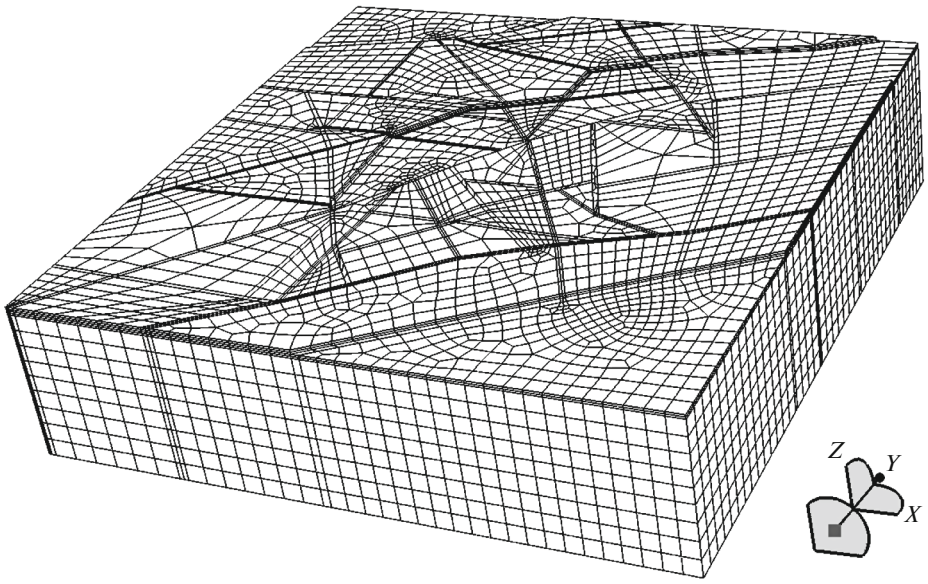

Fig. 7. Model of terminal elements created for 3D analysis of stressed state of upper crust, which host SUOFs. Axis Y points to north.

suggested that the lack of a lateral bearing reaction of the external tectonic structures is partly compensated by the terminal displacements along faults in the horizontal plane.

Nevertheless, the influence upon the wedge-shaped block of the North Khingan TB in most of the calculation variants (A–E), beginning from the second step of loading, gave rise to the localization of the influence in the zone limited by the marginal NW–SE-trending fault and the eastern lateral boundary of the model. The model collapsed at the third or fourth steps of loading in almost all the indicated cases.

Because of the inheritance of the spatial distribution of the analyzed characteristics for revealing the most probable scheme of tectonic loading, we are content to consider the calculation results only for the first step of loading, assuming that a plastic flow is realized in the geological medium only along faults without large deformations and without a discontinuity of model. Simulation has been carried out for Ten variants of the marginal loading conditions were simulated (Table 2).

A short description of the loading variants is given below. *Variant of load A:* the corner blocks are displaced under the vertical load along the boundary faults. It is evident that this type of loading satisfies setting the left-lateral strike-slip boundary faults, as well as the suggested axial compressive load in the near-meridional direction. Under the chosen conditions of fastening (free surfaces along the boundaries and orthogonal boundaries of load application), it is evident that the northeastern and the southwestern corners of the model will occur in the extension setting and that here deformations will be realized through the increase in the block volume. This is corroborated by the distribution of the Lode-Nadai coefficient and the zeroth maximal tangent stresses in the indicated domains. The distribution of the tangential stresses points to the activity of faults in almost all directions, albeit, only within the zone affected by loading. Consideration of the Lode-Nadai coefficient makes it possible to rank the selected fault systems into two types: (i) relative volumetric compression in the NE–SW fault zones and (ii) setting of extension in the NW–SE fault zones. Taking into account that the conventional Lode-Nadai coefficient shows a type of stress tensor in the form of triaxial strike-slip–compression, the obtained pattern may be interpreted as follows: strike-slip develops along the NE–SW faults, whereas the extension setting in the NW–SE faults activates them. The comparison of the orientation of the principal stress axes with the mechanisms of the stressed state in the SUOF, determined by the morphostructural method, does not reveal satisfactory coincidence.

A variant of load B was applied in conditions when horizontal displacements on the vertical boundaries of loaded blocks could not be attained. This regime leads to a more strongly expressed displacement of the loaded wedges in vertical directions, as indicated by the elevated amplitudes of the displacements near the vertical lateral boundaries (in the plane of a sheet of paper). The minimal displacements are localized in the area extending in the NNE–SSW direction with two clearly expressed minimums symmetrically located relative to the NE–SW-trending diagonal fault. The parallel faults largely possess a stress tensor in the form of triaxial strike-slip–compression, whereas a strike-slip tensor with a component of the

Table 2. Variants of marginal loading conditions for 2D simulation

Variant	Brief characterization of loading mode and simulated process
A	Vertical pressure on TB boundaries at free lateral boundaries. Simulation of block displacement along restrictive regional faults
B	Vertical pressure on TB boundaries at fixed lateral boundaries. Simulation of absence of horizontal block displacement
C	Vertical pressure from side of North Khingan TB at fixed other lateral boundaries. Simulation of absence of displacement along block boundaries
D	Vertical and horizontal pressure on lateral TB boundaries. Simulation of regional compression in NW–SE direction
D1	Vertical and horizontal pressure on lateral boundaries of North Khinhan TB in combination with vertical pressure and horizontal displacement of Gazimur–Klichka TB. Simulation of non-coaxial regional compression
E	Vertical pressure on boundaries of North Khingan and Gazimur–Klichka TB at oppositely directed displacements of lateral boundaries. Simulation of counterclockwise torsion compression, i.e., NE–SW regional compression in general
F	Superfluous loading on northern boundary of Gazimur–Klichka TB in combination with compressive loading on other boundaries. Simulation of coaxial regional compression and compression in Klichka Fault Zone
F1	Superfluous loading on northern boundary of Gazimur–Klichka TB in combination with compressive loading on other boundaries. Simulation of coaxial regional compression and compression in Klichka Fault Zone
F3	Superfluous loading on northern boundary of Gazimur–Klichka TB in combination with horizontal displacement of lateral boundary. Simulation of noncoaxial regional compression and left-lateral with displacement along Klichka Fault
F5	Superfluous loading on northern boundary of Gazimur–Klichka TB in combination with compressive loading on other boundaries. Simulation of coaxial unilateral displacement of blocks

single-axis extension occurs in the orthogonal system of the NW–SW-trending faults. This implies that in comparison with the preceding loading variant, in this situation, the system of NW–SE faults is activated due to the strike-slip offset along the main NE–SW-trending faults. Despite the qualitatively valid pattern of the fault's kinematics, the comparison of the calculated orientations of the principal stress axes with those reconstructed using the morphostructural method did not yield a good correlation: along with the coincidence in the local areas, where the extension setting is determined, in most cases deviations in the orientation were ~40°.

The variant of load C represents the lateral prop for displacing North Khingan TB on the assumption that there are no horizontal displacements to the northwest of the fault zone along the Argun River. The effect of the pressing block initiates the main displacements in the eastern part of the simulated area, making up stretching deformations along the NW–SE-trending and near-meridional faults, i.e., along the direction of load application. It is evident that the lug formed by the immobile block from the side of the Klichka Fault gives rise to the appearance of a high-pressure domain and to compression in the near-latitudinal faults. Despite this, significant tangential stresses arise along these faults and give rise to the realization of a stress tensor in the form of a triaxial strike-slip–compression. The coincidence in the orientation of the main principal stress axes is observed, as in the preceding case, in the areas of a local extension. It should be noted that good coincidences are related to the main NE–SW faults. In other areas, the orientations of the maximal compressive stresses differ by ~45°.

In the *variant of load D,* it was noted that in the case of loading set over one step, the smallest displacements in the amplitude are observed in the central part of the model, while the paths of the displacements spread outward from this stable area. All NE–SW-trending faults are characterized by the elevated values of the maximal tangential stresses as evidence of their activation. The near-latitudinal faults were also activated. In general, the distributions of the tangential stresses are correlated with the distribution of the maximal strike-slip deformations, which are predominant. The NW–SE faults are characterized by achieving the maximal tangent stresses and 3D elasto-plastic deformations. In the case of weak tangential stresses and lower pressure compared with the enclosing rocks, negative 3D deformations are observed here. This is evidence of the setting of an extension in the NW–SE faults. A comparison of the Lode-Nadai parameter and the calculated orientations of the principal stress axes with the orientation of the neotectonic stresses

indicates their substantial divergence, despite the quality of the reproduced activity of the NE–SW fault system.

In the *variant of load D1,* the corner blocks move in the diagonal direction shown in Fig. 8 rather than along the bounding faults. This is indicated by the maximal levels of the displacement amplitudes. The distribution of the pressure shows that its elevated levels are related to the setting of marginal conditions. In the NE–SW-trending diagonal fault zone, the influence of such a type of compression is combined with minor pressures in the southwestern and northeastern parts of the model.

It is evident that on the prolongation of the model structures in the NE and SW directions, the area of stress formation will be wider, whereas the domains of the lowered pressures in the mentioned areas may be removed beyond the boundaries of the considered structure. The distribution of the tangential stresses shows that the faults oriented in almost all directions remain active within the zone affected by loading. The consideration of 3D deformations (Fig. 8e) allows us to establish two types of fault kinematics. For the NE–SW-trending and near-latitudinal faults, the relative 3D compression is recorded, whereas for the NW–SE-trending and near-meridional faults, the setting of extension is typical. Taking into account the Lode-Nadai coefficient, the NE–SW-trending faults are characterized by a stress tensor in the form of a triaxial strike-slip–compression, and this allows us to interpret the pattern obtained as follows: the NE–SW-trending zones are characterized by strike-slip faulting, whereas extension in the NW–SE-trending zones activated them. The correlation of the orientation of the principal stress axes with the projections of the orientation of the principal stresses calculated with the morphostructural method reveals good conformity. Some inconsistencies may be caused by the circumstance that in the 2D setting the algebraically middle stress should be a priori oriented vertically relative to the model's plane and the algebraically minimal principal stress should be tensile, whereas according to the morphostructural method, all three components of the principal stress tensor actually occur.

A comparison of the displacement amplitude distribution in the *variant of load E* with the variants analyzed earlier showed that the domain with the smallest displacements of the surface is stretched in the NE–SW direction. This allows us to speak about the possible origination of the extension setting in the domains with the minimal amplitudes of the horizontal displacements. As in variant D1, the distribution of the maximal tangential stresses provides evidence of the activation of the NE–SW-trending faults. The 3D deformations also allow us to suggest a sliding apart of the NW–SE-trending faults. Comparing the calculated projections of the principal stresses on the horizontal plane also yields satisfactory correspondence. The good coincidence of the domains with extension settings is noted. The main deviations in the orientation are observed in the domains, where the triaxial tension state has been interpreted. The conformity of this parameter for the load variant E is somewhat worse than that for the load variant D1.

In all the aforementioned variants, the lack of an additional lateral prop at the vertical (in the plane of a sheet of paper) boundaries leads to a shortage of pressure in the southwestern and northeastern corners of the model. On the one hand, this gives rise to the appearance of an extension setting in these domains and the formation of stress tensors in the form of a triaxial shear–compression in the NE–SW-trending faults. On the other hand, the matter spreads through the free boundaries. In particular, such a situation is permanently observed in the northeastern part of the model.

In order to overcome this circumstance, in the *F1 series of loadings,* it was assumed that on application of a load to the northern boundary, the near-latitudinal Klichka Fault was a boundary of the pressing tectonic block (Fig. 6).

In the *variant of load F,* the maximal pressures and tangential stresses in the fault zone are established in the northeastern part of the model. If we compare the distribution of the maximal tangential stresses and the Lode-Nadai coefficient, we may note that the compression setting is established in the central part of the model, along with the minimal tangent stresses. A comparison of the orientations of the principal stress axes yields unsatisfactory compliance.

If the opposite blocks to which load is applied undergo similar counter displacements (the *variant of load F1*), then the domains of the elevated and lowered pressures are divided by the NW–SE-trending fault in the central part of the model. In this case, the pressure values observed in the NW–SE faults are negative and these faults open even in high-pressure domains. A negative 3D deformation is also noted in them. The correlation of the principal stress axes also does not give satisfactory results.

In the *variant of loading F3,* the elevated pressure values in the northwestern part of the model are similar to those in the preceding two cases and caused by the influence of the North Khingan Block, to which a load with a significant meridional constituent is applied. The distribution of the Lode-Nadai coefficient barely differs from variant F. The elevated values of the maximal tangential stresses are observed practically in all the fault systems except for the largest NW–SE-trending faults. Note that the correlation of the orientations of the principal stress axes with the characteristic settings of the local stressed conditions is in general satisfactory. Divergence of the latter criterion is established only in the northwestern part of the model and estimated at ~45°.

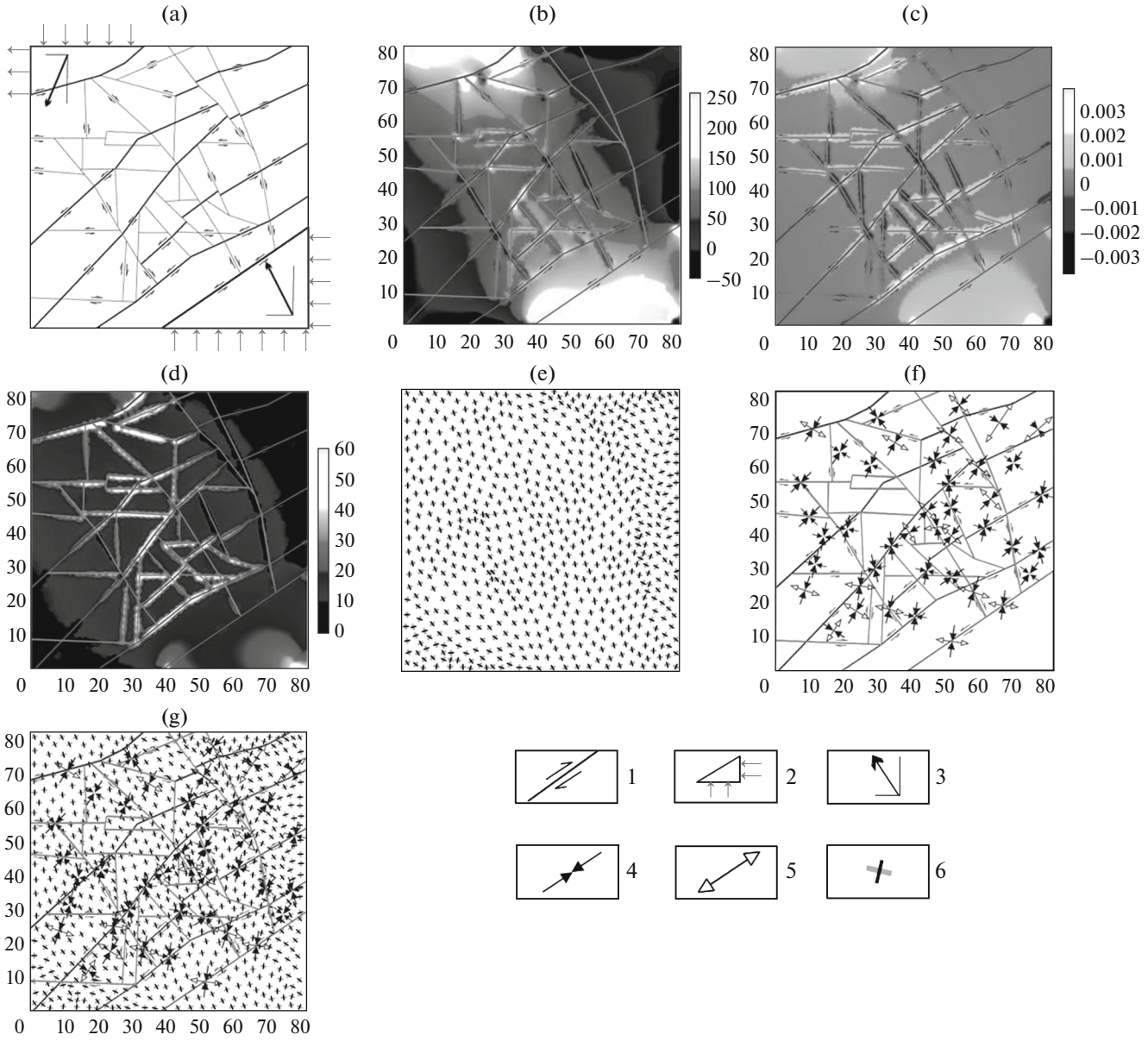

Fig. 8. Influence on 2D model set by marginal loading conditions (variant D1): simulation of not coaxial regional compression under vertical and horizontal pressure on lateral boundaries of North Khingan Tectonic Block in combination with vertical pressure and horizontal dislocation of Gazimur–Klichka Tectonic Block: (a) scheme of loading; (b) tectonic pressure, MPa; (c) 3D deformations (relative values); (d) maximal tangent stress, MPa; (e) map of principal normal stress paths (algebraically maximal and minimal); (f) fault network with indication of fault zones and orientation of principal stresses at neotectonic stage established with morphostructural method; (g) resultant pattern of juxtaposed models (e) and (f). (1) main faults and displacement directions of their limbs; (2) direction of influence on model blocks; (3) resultant direction of block displacement; (4) axes of principal compressive stresses determined from results of morphostructural analysis of tectonic stress field; (5) axis of principal tensile stresses determined from results of analysis of tectonic stress field by means of morphostructural method; (6) axes of maximal principal compressive stresses (black segments) and minimal compressive or tensile stresses (gray segments).

The variant of loading F5 gives the expected pressure and Lode-Nadai coefficient distributions. The extension setting with insufficient pressure (slightly negative values up to 30 MPa) and the lowest values of shear deformation are noted in the northwestern part of the model (Gazimur–Klichka TB). However, in general, the coinciding orientation of the principal stress axes is extremely rare. According to the geological and tectonic data, the compression mechanisms differ by –60° to –40°.

Thus, the analysis of ten loading variants in 2D simulation shows the following points. To ensure the setting of the left-lateral strike-slip fault extending along the Argun River valley, it is necessary that the

action should be compressive and have a positive NE–SW component along the strike of the fault. This influence is provided by loading the North Khingan TB in the southeastern corner of the model. It is expedient to constrain the Gazimur–Klichka TB situated in the northwestern corner of the model by the near-latitudinal Klichka Fault. This allows us to realize a supportive reaction from the aforementioned boundary. In the presence of the compressive influence and the southern component, this support gives rise to the formation of a domain affected by loading, which encompasses a significant part of the model. Taking into account the fact that the NE–SW-trending fault system is the youngest, we can expect the shearing or transtension setting in the aforementioned faults. Such a situation is observed in loading variants C, D, D1, F3, and F5 in contrast to the system of older NE–SW, near-latitudinal, and near-meridional faults.

The best conformity of the orientation between the projections of the principal stress axes and the results of the determination of the stressed state with the structural–geological method has been established for the loading variants C, D1, and F3. In these variants, the axial compression is predominant, and this corroborates the initial hypothesis about the leading role of this mechanism of loading. Nevertheless, in contrast to variant D of loading, where the direction of the axial compression has certain northwestern constituents, the aforementioned three variants realize the possibility of squeezing the material to the west (to the left in the plane of model).

The setting of the horizontal extension determined by the morphostructural method in the northeastern part of the model and those observed in the loading variants C, D, D1, and F5 may correspond to the opening of the intermontane Sukhoi Urulyungui Basin. Variants D and F5 show a very weak conformity of the convergence criterion with the results of determining the stressed state with the structural–geological methods. In variant F3, which displays the best coincidence with this criterion, conditions for an extension in the basin were not identified. For the NE–SW-trending fault systems, the shear or transpression setting is clearly expressed practically everywhere. In variants C, D, and F3, the nearly latitudinal faults (e.g., the Klichka Fault) reveal a similar activity. Note also that determination of the extension setting in the northeastern part of the model is, in general, consistent with the calculated orientations of the principal stresses in the loading variant D1. It should be taken into account that a number of determinations (Petrov et al., 2010) obtained with the morphostructural method may be linked to the realization of strike-slip offsets along the near-meridional faults, whereas the other part, which occurs in good correspondence with the calculated data, is in accordance with the faults of a lower rank and may be related to tectonic stresses within blocks.

To create the correct model of loading evolution, the representative information on ancient dislocations and the changeable regional stress field over geological time, e.g., since the Paleozoic, is needed. The above-mentioned parameters may be obtained from the analysis of slickenlines, using the cataclastic analysis of fractures (Rebetsky, 2011), or with the method of strain analysis (Voitenko, 2000, 2008).

As has been established as a result of research studies, to realize lateral support at the northern and western boundaries of the model, it is expedient to set marginal conditions which prevent the material from spreading. When the loading at the northern and southern boundaries of the model is set, it must take into account the possibility of the material being squeezed in the western direction; this ensures the setting of an extension in the northeastern part of the simulated territory (the northeastern part of the Sukhoi Urulyungui Basin). These suggestions have been implemented in the tectonic loadings of the triangular model.

Results of 3D Simulation

The construction of the 3D model of the DM of rock massifs is the next stage of geological–structural analysis and geodynamic simulation of geological structures in the area of the SUOF. Taking into account the assumption accepted in accordance with Fig. 5, the 3D model was constructed on the basis of the parameters inherent in geomaterials (Table 1) and the framework of fault tectonics (Fig. 6) for which the network of terminal elements was constructed (Fig. 7).

The differences in topography were accounted for as follows: for central (Sukhoi Urulyungui Basin), southeastern (Agun River valley), and northwestern (West Urulyungui Basin) parts of the model, the height of the surface was taken to be 500 m above the conditional sea level (zeroth) level. The sedimentary and volcanic rocks occur deeper (down to the zeroth spot elevation). The remaining heights were assumed to be 1 km and were correlated with the granitoid massifs; thin units of sedimentary and volcanic rocks have been omitted.

The loading schemes are shown in Fig. 9. The following conditions were used as the initial fastenings:

—On the lower plane bordering the model from below (depth, 20 km) all the nodes are fixed (there are no displacements or turns);

—Ot the lateral boundaries, displacement along vertical axis (Z) is accepted;

—Along the X and Y axes located in the horizontal plane, displacements are accepted to be zeroth displacements;

—The upper surface is free of fastening.

The implementation of the 3D loading model is put into effect as follows:

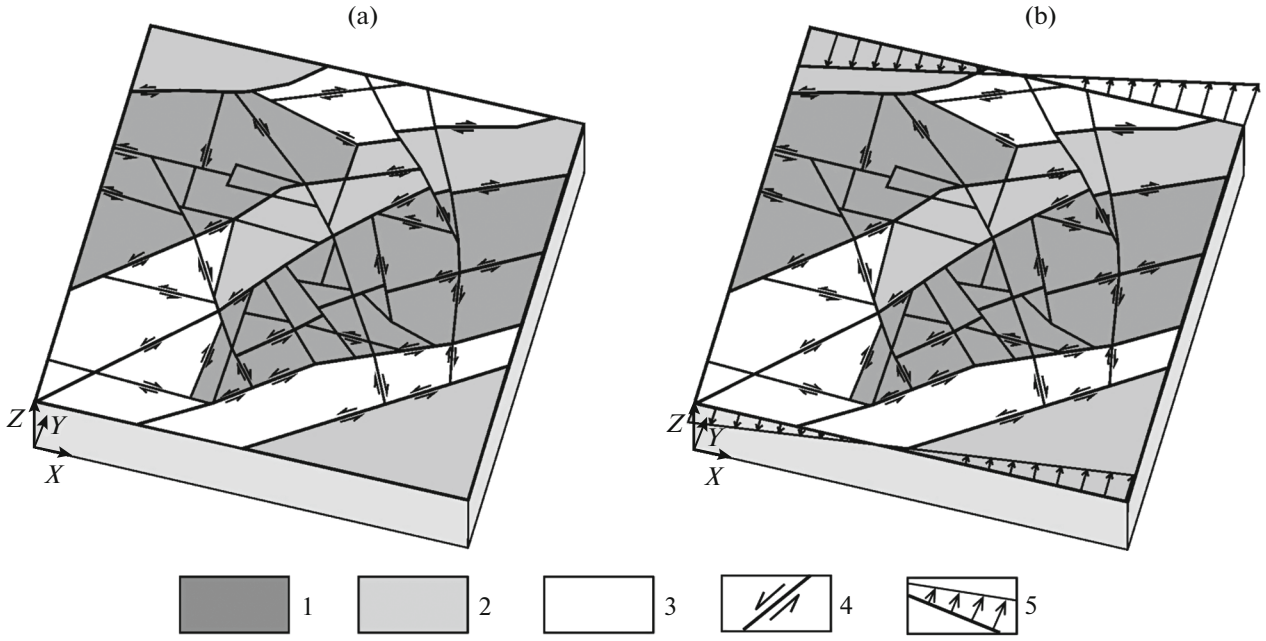

Fig. 9. Main schemes of loading for 3D model of DM of rocks in Strel'tsovka ore field: (a) takes into account initial gravitational stress state and additional ascent of granitoid masses and (b) takes into account load created by horizontal tectonic forces, giving rise to extension in central part of model. (1) domains with vertical uplift of surface; (2) domains with height of 500 m; (3) domains with height of 1000 m; (4) faults and direction of displacement of their limbs; (5) direction of horizontal displacements in simulated volume.

—The gravitational DM was formed at the first stage;

—The rise of the surface (domains of mountain edifices, Fig. 9) was simulated at the second stage by application of the vertical load;

—The shift of the lateral surfaces was set at the third stage.

The 3D geodynamic simulation was carried out for loading under its dead weight. The latter is understood as the formation of the initial stressed state under the effect of gravity. Taking into account the compressibility of the geomaterials and criterial possibility of a domain's transition into the plastic flow, the internal damages, deformations, and stresses are gained at the given step due to the features of the internal structure in the absence of external forces.

To simulate the effect of ascending movements in the areas of mountain edifices (Fig. 9a), vertical displacements with an amplitude of 60 m are set within the projection of their boundaries on the lower horizontal plane. This approximately corresponds to the sagging of the surface in these areas during the formation of the model of the initial stressed state under the effect of the dead weight of the rocks calculated at the preceding loading step.

The amplitudes of the horizontal displacements were in the ratio of 2 : 1. The maximal amplitude of the displacements at the southern (lower in the plane of the figure) and the upper (northern) boundaries were 100 and 200 m, respectively. Thus, a relative extension was created in the northeastern part of the model and a relative compression in its western part. At the stage of load application, the displacements in the north–south direction (along the Y axis) were "resolved" at the eastern and western boundaries.

The loads were applied in one step.

The problem, without accounting for the uplift of the mountain domains composed of granitoids, was computed for the sake of comparison (Fig. 9b). Thus, the relative extension (imitation of the opening of the Sukhoi Urulyungui) was created in the eastern and central parts of the model and the relative compression in the western part of model.

Sixteen variants of the parameter–process combinations (Table 3) were analyzed during the 3D simulation. An example of simulation (variant 4) is shown in Fig. 10.

The distribution of the pressures by depth in the problem concerning the effect of gravity on the formation of the initial gravitation state shows that the local regions of the confined pressure shortage are observed on the surface and then completely disappear at the conventional sea level. They give way to regions of the minimal compressive pressure, being divided by the connected regions of a relative increase in pressure up to 40 MPa. Note that during simulation the heterogeneities of the topography were represented by local plateau-type elevations with the central Sukhoi Urulyungui Basin, the western part of the Gazimur–

Table 3. Parameters and processes analyzed in course of 3D simulation

Variant	Brief characterization and simulated process
1	Dead weight: pressure distribution in depth, MPa
2	Dead weight: distribution of maximal tangent stresses in depth, MPa
3	Dead weight: distribution of displacement amplitudes, m
4	Dead weight: intensity of maximal main elasto-plastic deformations, nondimensional
5	Dead weight and uplift (without shear): distribution of pressure, MPa
6	Dead weight and uplift (without shear): distribution of maximal tangent stresses, MPa
7	Dead weight and uplift (without shear): distribution of displacement magnitudes, m
8	Dead weight and uplift (without shear): distribution of maximal elasto-plastic deformation magnitudes, nondimensional
9	Dead weight, uplift and shear: distribution of pressures, MPa
10	Dead weight, uplift and shear: distribution of maximal tangent stresses, MPa
11	Dead weight, uplift and shear: distribution of displacement magnitudes, m
12	Dead weight, uplift and shear: distribution of maximal elasto-plastic deformation magnitudes, non-dimensional
13	Dead weight and shear (without uplift): distribution of isotropic pressures, MPa
14	Dead weight and shear (without uplift): distribution of tangent stresses, MPa
15	Dead weight and shear (without uplift): distribution of displacement magnitudes, m
16	Dead weight and shear (without uplift): distribution of intensity of shear elasto-plastic deformation amplitudes, non-dimensional

Klichka TB, and the South Argun Basin (valley of the Argun River) deepened by 500 m.

The central basin is characterized by the background pressure level to a depth of 2 km. Further, to a depth of 5 km, the level of the measured pressure is lower by ~20 MPa than in the host granitoid framework. Still further the central basin is not expressed in the pressure field at all the analyzed levels. Note that in general pressure grows monotonically with depth due to the elevated incompressibility of the model's geomaterials in the fault zones. This probably implies the following points:

—In the given situation, with the absence of substantial lateral pressure gradients, this parameter is close to lithostatic;

—The lowered pressure values in the central basin can be treated as a result of the additional squeezing of the basin under the effect of isostatic compensation, which is induced by mass redistribution due to the additional load related to the positive landforms;

—The heterogeneous distribution of the pressures is expressed at the upper levels of the structure under consideration; then, they are expressed weaker downward, and at a depth of 2 to 3 km the pressure field becomes relatively homogeneous.

The distribution of the tangential stresses in the models shows that the given parameter gradually increases with depth from the zero values on the surface to ~120 MPa at a depth of 7 km. It should be noted that the central basin expressed as a gradient of the tangential stresses is clearly exposed at two depth levels. It is weakly expressed on the surface, but is distinctly marked at the absolute zeroth level. Further it is not expressed down to a depth of 3 km and further decreases giving way to zones of the local maximum tangential stresses along the faults and within small blocks as evidence of the increasing significance of shearing in the formation of the general DM of the deformation. Thus, above the level of 3 km (conditionally), deformations are primarily generated either by 3D compression or extension, whereas at deeper levels, shearing largely participates in the redistribution of stresses.

Although it is difficult to judge the character of the accompanying processes from the amplitudes of the displacements, we nevertheless note the following points. As the granitoid complex in our model is underlain by a structural (model) layer with lowered compressibility and elevated fluidity, it can be stated that vertical sagging will make the main contribution to the amplitude of the displacement. Indeed, these amplitudes are maximal in the regions of elevated topography. As was discussed above, the gravitational effect of mountain edifices in this case is higher and gives rise to greater 3D compression here and an ele-

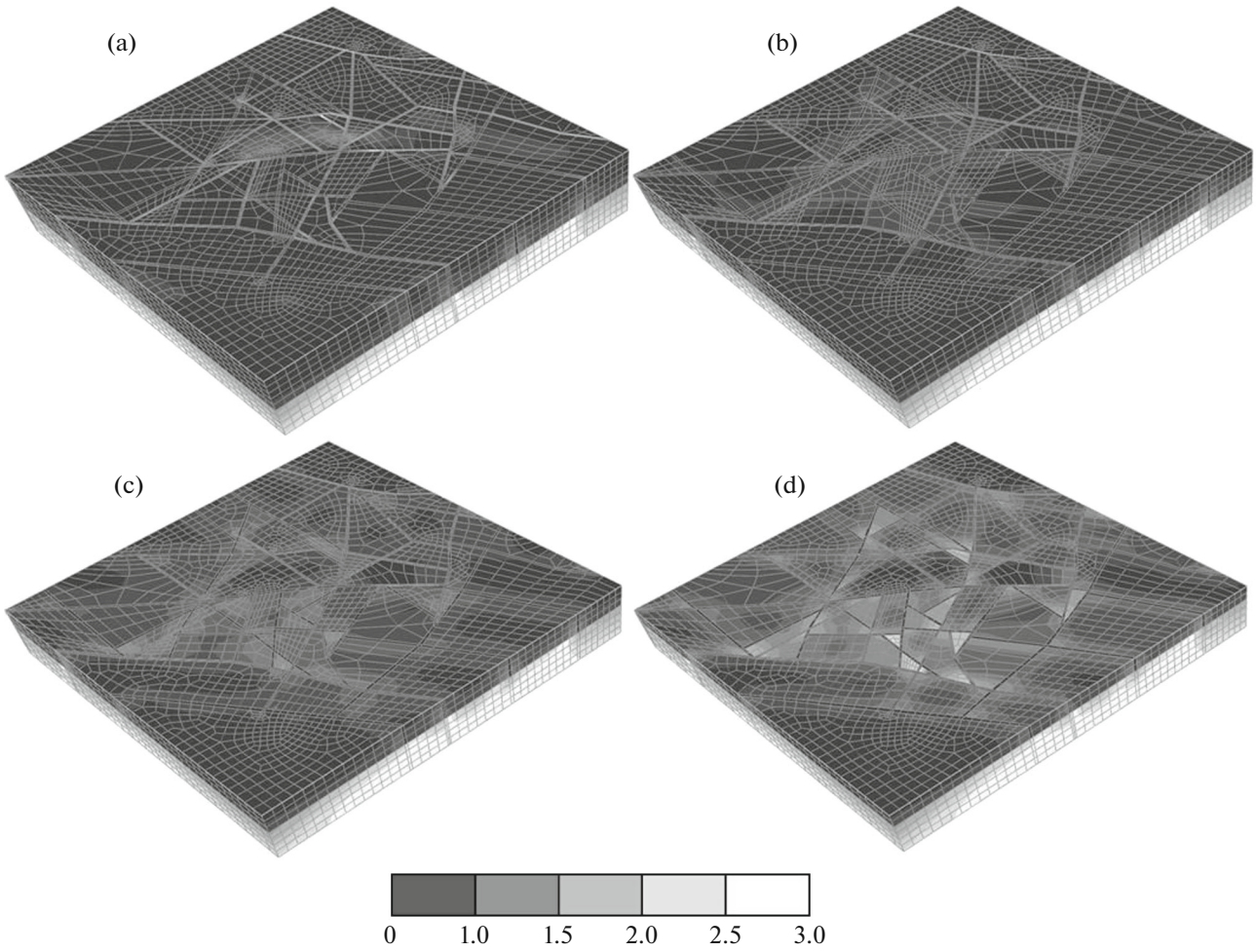

Fig. 10. Calculated intensity (from 0 to 3) of maximal principal elasto-plastic deformations (Table 3, variant 4) at various depths of geological section: (a) 0 km, (b) –2 km, (c) –4 km, (d) –6 km. Conditions of loading have been determined by dead weight of rocks.

vated load at the underlying structural levels. The formation of a local region in the eastern part of the model (the area close to the Dosatui Settlement) should also be noted. This region is traced from the surface to a depth of 7 km, making up a conic structure. The displacement amplitudes in the central basin yield similar values in the depth range from the surface down to 5 km. The lack of dynamics here is clearly related to the effect of the lateral support that occurs under the effect of the gravity anomalies formed by the mountain uplifts in the area occupied by the granitic rocks.

The distribution of the intensities of the maximal main elasto-plastic deformations shows that, in the upper units, the highest values within the tectonic blocks are reached in the sedimentary cover of the central basin. This is probably caused by the initial strength of the sedimentary and volcanic-sedimentary rocks, which undergo squeezing, as a supplement to the setting of the predominant vertical compression under the effect of gravity. One kilometer below sea level, the elevated values of this parameter acquire a zonal character. The region of their manifestation covers the central part of the model, including the southwestern end of the Sukhoi Urulyungui Basin and the area of Strel'tsovka Caldera. Below a depth of 3 km, the maximal elasto-plastic deformations are attracted to the NE–SW-trending faults. The maximal values at these depths are noted in the small blocks bounded by the NW–SE-trending faults. This pattern is inherited by the distribution at a depth of 5 km with the striking differentiation of small blocks. The same pattern is also observed at a depth of 7 km. The maximally achieved values are localized here in the adjoining faults, which converge at acute angles. It should be noted that the smallest deformation values are observed beneath the Sukhoi Urulyungui Basin, whereas the linear zone along the Klichka Fault is characterized by an elevated level of deformations.

The formation of an additional rise of granitoid complexes results in the leveling of the pressure at a depth greater than 1 km in the southwestern part of the basin. The area of the maximal elasto-plastic deformations is localized beneath the granitoid complex adjoining the Argun River valley. The significant elasto-plastic deformations also rim the Gazimir–Klichka Tectonic Block and mark the meridional faults to the west of the Sukhoi Urulyungui Basin, where they are also traced in the upper units of its southeastern part.

The analysis of the effect of the tectonic strike-slip fault at the next loading step shows that, in the aforementioned model, a significant extension in its northeastern part is formed, being limited by the master NNE-trending fault. The additional pressure from the side of the western segment of the Gazimir–Klichka Tectonic Block is probably compensated by the boundary ESE-trending strike-slip faults and meridional faults occurring nearby. The smallest values of the maximal tangent stresses correspond to the cluster of small blocks in the granitoid complexes to the south of the Sukhoi Urulyungui Basin. In addition to the above-listed features, the distribution of the maximal elasto-plastic deformations is also evidence of the activation of the NE-trending faults. It is assumed that these faults, which bound the granite complexes and basins, could have been formed at the stage of the rising intrusive masses. As a result, the structure of the echeloned normal faults striking in the northeastern direction, as well as the near-meridional crosscutting normal and reverse faults could have been formed (Petrov et al., 2010). The implementation of the proposed loading scheme is also supported by the character of the displacements established on the basis of GPS, which points to the opening of the Sukhoi Urulyungui Basin.

The solution obtained without a vertical rise of the granitoid massifs at the stage of the initial stressed state but taking into account the proposed mechanism of the tectonic effects reveals a similar influence on the eastern part of the model. Here, however, this mechanism results in the activation of the strike-slip offsets along the near-meridional faults and in a tendency to a closure of the Sukhoi Urulyungui Basin.

DISCUSSION

The largest and unique mineral deposits, including those of strategic types of mineral commodities (gold, uranium, rare metals, etc.), were formed in the geological past in the activated mobile belts at the boundaries of stable lithospheric blocks (*Fundamental'nye ...,* 2012). At present, these ore-bearing zones are characterized by elevated tectonic disturbance and seismic activity (*Ekstremal'nye ...,* 2011).

At the operating deposits, under the conditions of a gradual shift of the mining front toward deep levels, the manifestation of rock pressure, along with the geodynamic processes, is activated. Their combination frequently gives rise to a rock burst (bump), or technogenic earthquakes of a destructive force (Adushkin and Turuntaev, 2005; Kurlenya et al., 2005). In Russia and the rest of the world dozens of such phenomena have been recorded: mines at the Lovozero rare-metal deposit, the Tashtagol iron deposit, the North Ural bauxite mines (*Katalog ...,* 1989), the Lockerby Ag–Pb–Zn deposit in Canada (Urbancic and Trifu, 1998), etc. As a result, the mines are compelled to stop operations, occasionally for a long time. In conditions when the surrounding town is formed around the mining enterprises, this leads to negative social–economic consequences.

In the past decades, the networks for monitoring tectonic events and the deformation of lithospheric blocks have become important instruments in the solution of basic scientific and applied problems, which have a special importance for the national economy and for protection against accidents. One such example is the system of stations that monitor seismotectonic processes in the Baikal Geodynamic Ground created at the end of the 20th century and that covers the South Baikal region, the Eastern Sayan, Tuva, and central and western Mongolia (San'kov et al., 2005; Lukhnev et al., 2010). The results of research in this territory helped form the decision to change the route of the East Siberia–Pacific Ocean pipeline away from the Baikal Rift System in which contemporary seismotectonic activity is developing intensely .

Nevertheless, such a monitoring system focused on the present-day geodynamic and seismotectonic processes does not exist in the vast territory of the southeastern Transbaikal region adjoining the Baikal Rift in the southeast. This is indicated by the World Stress Map Project—the global GIS—which currently combines 22000 worldwide constant and temporary observation points which monitor deformations in the lithosphere (Reinecker et al., 2005).

Along with this, the large ore clusters and fields, which are localized in the territory of the southeastern Transbaikal region, have historically been leading suppliers of strategical mineral commodities such as gold, uranium, and rare metals (Bortnikov et al., 2012). The further prospects of mining in Transbaikalia are related to the following factors:

—Propagation of the mining front to the deep levels of operating deposits against a background of complicated mining and geological conditions;

—Commissioning new large deposits, whose mining and geological conditions remain uncertain.

To ensure the development of mineral resources, it is necessary to assess the geodynamic and seismic settings on the common geoinformational platform, to implement the 3D simulation of the geological and tectonic structures and the evolution of contemporary seismogeodynamic processes, as well as to work out

the infrastructure of networks monitoring the displacements on the Earth's surface and seismotectonic events in the lithosphere of the mining territories. The subsequent arrangement and commissioning of these networks must ensure the efficiency of the planning and implementation of enterprises focused on rational mining management and the environmental safety of the operating and new mining complexes.

In the context of creating a geoinformational platform, the following points need to be carried out:

—Systematize information on the spatiotemporal heterogeneity of the stress field and dynamics of the formation of a fault's tectonic elements and mechanisms of stress generation in lithospheric blocks;

—Organize work with the geodata bases and topographic, geological, tectonic, ore-forming, hydrogeological, and other map materials in a common coordinate system;

—Create 3D geoinformational models of the geoogical and tectonic structures of the territory and development of seismogeodynamic processes in separate blocks of the Earth's crust with the recognition of seismically active areas and fault zones;

—Elaborate GIS projects of the geodynamic ground with the establishment there of points assigned to monitoring the Earth's surface movements and seismogeodynamic processes, taking into account the geological and tectonic structures of the territory that is promising for developing mineral resources and in terms of its social–economic potential.

According to the results of the analysis of the spatiotemporal development of the seismogeodynamic processes and DMs of rock massifs, the conceptual and numerical models should be elaborated in various scales (regional, transitional, local). The simulation results should be verified by the data of field observations using seismoacoustic, seismodeformational, and other methods of information acquisition in situ; the proposals for localizing the points assigned for monitoring the natural and technogenic processes should be stated.

These undertakings are currently being implemented in Krasnokamensk by PAO PPGKhO, which mines and processes uranium ore from deposits of the Strel'tsovka ore field that have unique reserves.

In addition, the integrated 3D model of the DM of the geological medium presented in this paper may be used to forecast the potential ore reserves at the deep levels and flanks of the deposits. This procedure is implemented by retrospective analysis based on the reconstruction of the tectonodynamic formation conditions of ore-bearing structures in the deposits and the paleotectonic state of the rock massifs, taking into account their rheology and dynamics of fluid-generating physicochemical processes. In combination with the modern structural–geological, structural–petrophysical, and tectonophysical methods, including the quantitative computation of stresses and deformations (Petrov et al., 2015), there is a possibility to establish migration paths and determine the concentration conditions of the valuable components in the ore formation zone.

CONCLUSIONS

The main results of the research in the area of the production activity of PAO PPGKhO, the largest complex of mining and processing of uranium ore in Russia can be summarized as follows. The geological–structural analysis and geodynamic simulation of the geological structures of the Strel'tsovka ore field were carried out on the basis of newly elaborated schemes: (i) fault tectonics are based on the data of the geological–structural, mineralogical–petrographic, and petrophysical mapping of the main fault zones; (ii) the localization of seismodislocations is based on the results of their mapping and the structural–geomorphic analysis of the territory; and (iii) the distribution of the seismotectonic regimes (stress-tensors) is based on the data of the structural–kinematic analysis of the fault zones. All these materials have been combined into the common 3D GIS project based on the ArcGIS 10 platform with the ArcGIS 3D-analyst module.

For the first time, the rates and directions of present-day horizontal movements have been measured in the Strel'tsovka ore field using the GPS geodetic methods at permanent and temporary observation points. The averaged mechanism of earthquakes and orientation of the axes of the principal compressive and tensile stresses in this area have been determined.

Based on the geostructural, geophysical, geotectonic, petrophysical, and other data, we have created models of the structure, properties, and rheological links of a geological medium. The boundary conditions for numerical tectonophysical simulation have been determined using the method of terminal elements. The 2D and 3D models of the DM of rock massifs have been elaborated on the basis of the data on the present-day stresses and seismotectonic deformations with the selection of active faults. For the first time in our practice, the calculated geodynamic models have been integrated into 3D GIS.

The simulation results have been verified at the regional and local scale levels. At the regional level, the confirmation has been received by a detailed (including the sinking of dug holes) study of the Klichka seismodislocation—a fault zone which has been active from the middle Pliocene to the present day (~5 Ma). At the local level, the simulation results are corroborated by the data of multiyear deformational and seismoacoustic monitoring of highly stressed massifs of rocks at the operating Antei molybdenum–uranium deposit. The good convergence of the results of the geodynamic simulation and observations in situ allows us to propose proceeding with a complex study of the paleotectonics and the recent

DM of rock massifs, with the focus of the research on the intracaldera part of the Strel'tsovka ore field.

ACKNOWLEDGMENTS

We thank A.V. Ponomarev, Yu.O. Kuz'min, E.A. Rogozhin, and L.A. Sim (Institute of Physics of the Earth, Russian Academy of Sciences, Moscow); and A.V. Parfeevets, and A.V. Lukhnev (Institute of the Earth's Crust, Russian Academy of Sciences, Siberian Branch, Irkutsk); A.N. Vlasov and D.B. Volkov-Belgorodsky (Institute of Applied Mechanics, Russian Academy of Sciences) for their consultation and assistance in setting problems and carrying out the spatiotemporal analysis of geodynamic processes, seismicity, surface displacement, stress, and deformation fields. We are grateful to B.A. Prosekin and S.I. Shchukin (PAO PPGKhO, Krasnokamensk) for their longstanding collaboration and assistance in resolving the questions mentioned in this paper. The study was supported by Program I.4P of fundamental research of the Presidium of the Russian Academy of Sciences, the Russian Foundation for Basic Research (project no. 15_05_01369_a), and the Russian Science Foundation (agreement no. 16-17-00018).

REFERENCES

Adushkin, V.V. and Turuntaev, S.B., *Tekhnogennye protsessy v zemnoi kore* (Technogenic Processes in the Earth's Crust), Moscow: INEK, 2005.

Andreeva, O.V., Golovin, V.A., Kozlova, P.S., et al., Evolution of Mesozoic Magmatism and Ore-Forming Metasomatic Processes in the Southeastern Transbaikal Region (Russia), *Geol. Ore Deposits,* 1996, vol. 38, no. 2, pp. 101–113.

Ben-Zion, Y., Properties of seismic fault zone waves and their utility for imaging low-velocity structures, *J. Geophys. Res.,* 1998, vol. 103, pp. 12567–12585.

Ben-Zion, Y. and Sammis, C.G., Characterization of fault zones, *Pure Appl. Geophys.,* 2003, vol. 160, pp. 677–715.

Bornyakov, S.A., Modeling shear zones on elastic–viscous models, *Geol. Geofiz.,* 1980, no. 11, pp. 75–84.

Bornyakov, S.A., *Physical simulation of lithosphere faulting at the modern stage: a review, Tektonofizika i aktual'nye voprosy nauk o Zemle. T. 1.* (Tectonophysics and Urgent Problems of Earth's Science)*, M.*: IFZ RAN, 2012, pp. 50–56.

Bortnikov, N.S., Petrov, V.A., Veselovskii, A.V., et al., Geoinformation System (GIS) of the Transbaikalian sector of the Mongol–Okhotsk Mobile Belt, *Rudy Met.,* 2012, no. 3, pp. 18–27.

Chester, J., Chester, F.M., and Kronenberg, A.K., Fracture energy of the Punchbowl fault, San Andreas system, *Nature,* 2005, vol. 437, pp. 133–136.

Chipizubov, A.V., Smekalin O.P., Imaev, V.S., Paleoseismodislocations in the Klichkinsk thrust zone, Southeastern Transbaikalia, *Voprosy inzhenernoi seismologii* (Problems of Engineering Seismology), 2014, vol. 41, no. 2, pp. 22–36.

Delvaux, D., Moyes, R., Stapel, G., et al., Paleostress reconstruction and geodynamics of the Baikal region, Central Asia. Part I: Palaeozoic and Mesozoic prerift evolution, *Tectonophysics,* 1995, vol. 252, pp. 61–101.

Delvaux, D., Moyes, R., Stapel, G., et al., Paleostress reconstruction and geodynamics of the Baikal region, Central Asia. Part II: Cenozoic rifting, *Tectonophysics,* 1997, vol. 282, pp. 1–38.

Dolgikh, G.I., *Issledovanie volnovykh polei okeana i litosfery lazerno-interferentsionnymi metodami* (Study of Wave Fields in Ocean and Lithosphere using Laser–Interference Methods), Vladivostok: Dal'nauka, 2000.

Dukhovskii, A.A., Amantov, V.A., Artamonova, N.A., et al., Seismic and gravity images of major ore districts and fields of the southeastern Argun' area (eastern Transbaikal Region, Russia), *Geol. Ore Deposits,* 1998, vol. 40, no. 2, pp. 87–99.

Eksperimental'naya tektonika v teoreticheskoi i prikladnoi tektonofizike (Experimental Tecctonics in Theoretical and Applied Tectonophysics), Luchitskii, I. V. and Bondarenko, P.M., Eds., Moscow: Nauka, 1985.

Ekstremal'nye prirodnye yavleniya i katastrofy. T. 2: Geologiya urana, geoekologiya, glyatsiologiya (Extreme Natural Phenomena and Catastrophes. Volume 2. Uranium Geology, Geoecology, and Glaciology) Gliko, A.O., Ed., Moscow: IFZ RAN, 2011.

Federal'nye normy i pravila v oblasti ispol'zovaniya atomnoi energii. Uchet vneshnikh vozdeistvii prirodnogo i tekhnogennogo proiskhozhdeniya na ob'ektakh ispol'zovaniya atomnoi energii (OIAE). NP-064-05 (Federal Norms and Rules in the Sphere of Application of Atomic Energy. Allowance for the External Natural and Technogenic Impacts on the Objects of Atomic Energy Application (OAEA). NP-064-05. (Fed. Sluzhba Ekol. Tekhnol. Atom. Nadzor, Moscow, 2005).

Fundamental'nye osnovy formirovaniya resursnoi bazy strategicheskogo syr'ya (Au, Ag, Pt, Cu, redkie elementy i metally) (Fundamental Principles of the Formation of Resource Base of Strategic Raw Material (Au, Ag, Pt, Cu, Rare Elements, and Metals), Bortnikov, N.S., Ed., Moscow: GEOS, 2012.

Geologicheskoe stroenie Chitinskoi oblasti. Ob"yasnitel'naya zapiska k geologicheskoi karte masshtaba 1 : 500000 (Geological Structure of the Chita Region. Explanatory Note to the Geological Map on a Scale of 1 : 500000), Rutshtein, I.G. and Chaban, N.N., Eds., Chita: GGUP Chitageols'emka, 1997.

Gintov O.B. *Polevaya tektonofizika i ee primenenie pri izuchenii deformatsii zemnoi kory* (Field Tectonophysics and its Application in Studying the Earth's Crust Deformations), Kiev: Feniks, 2005.

Gzovskii M.V. *Osnovy tektonofiziki* (Principles of Tectonophysics), Moscow: Nauka, 1975.

Instruktsiya po bezopasnomu vedeniyu gornykh rabot na rudnikakh i nerudnykh mestorojdeniyakh, ob"ektakh stroitel'stva podzemnykh soorujenii, sklonnykh i opasnykh po gornym udaram (RD 06-329-99) (Instruction on Safe Processing of Mining on Mines and Non-Ore Deposits and Underground Building Objects, Prone and Dangerous Relative to Rock Bursts (RD 06-329-99)), Moscow: GP NTTs Bezopasn. Promyshlen. Gosgortekhnadzora Rossii, 2000.

Ishchukova, L.P., Modnikov, I.S., Sychev, I.V., et al., *Uranovye mestorozhdeniya Strel'tsovskogo rudnogo polya v*

Zabaikal'e (Uranium Deposits of the Strel'tsovka Ore Field, Transbaikalia), Irkutsk: GK "Geologorazvedka", 2007.

Katalog gornykh udarov na rudnykh i nerudnykh mestorozhdeniyakh (Severoural'skoe, Tashtagol'skoe, Oktyabr'skoe (Noril'sk), Yuksporskoe, Kukisvumchorrskoe (PO "Apatit"), Kochkarskoe i drugie mestorozhdeniya (Catalogue of Rock Bursts on Ore and Nor-Ore Deposits (Severoural'skoe, Tashtagol'skoe, Oktyabr'skoe (Noril'sk), Yuksporskoe, Kukisvumchorrskoe (PO "Apatit"), Kochkarskoe, and Other Deposits) Leningrad: VNIMI, 1989.

Kochkin, B.T. and Petrov, V.A., "Long-term prediction for seismic hazard for radioative waste disposal," *Russ. Geol. Geophys.,* 2015, vol. 56, no. 7, pp. 1369–1380.

Kompleksnye geodinamicheskie poligony: metodika i rezul'taty issledovanii (*Complex Geodynamic Test Sites: Methods and Results of Studies*), Bulanzhe, Yu.D. and Lilienberg, D.A, Eds., Moscow: Nauka, 1984.

Komplekt kart obshchego seismicheskogo raionirovaniya territorii Rossiiskoi Federatsii (OSR-97) (Set of Maps of General Seismic Zoning of the Russian Federation (OSR-97)), Moscow: IFZ RAN, 1999.

Kurlenya, M.V., Seryakov, V.M., and Eremenko, A.A. *Tekhnogennye geomekhanicheskie polya napryazhenii* (Technogenic Geomechanical Stress Fields), Novosibirsk: Nauka, 2005.

Kuzmin, Yu.O., Tectonophysics and Recent Geodynamics, *Izv. Phys. Solid Earth,* 2009, vol. 45, no. 11, pp. 973–986.

Kuzmin, Yu.O. and Zhukov, V.S., *Sovremennaya geodinamika i variatsii fizicheskikh svoistv gornykh porod* (Recent Geodynamics and Variations of Physical Properties of Rocks), Moscow: MGU, 2004.

Lesne, O., Calais, E., and Deverchere, J., Finite element modeling of crustal deformation in the Baikal Rift Zone: new insights into the active-passive debate, *Tectonophysics,* 1998, vol. 289, pp. 327–430.

Lukhnev, A.V., San'kov, V.A., Miroshnichenko, A.I., et al., GPS rotation and strain rates in the Baikal–Mongolia region, *Russ. Geol. Geophys.,* 2010, vol. 51, no. 7, pp. 1006–1017.

Mikhailova, A.V., *Methodical problems of compilation and study of tectonic models using plastic equivalent materials, Eksperimental'naya tektonika: metody, rezul'taty, perspektivy* (Experimental Tectonics: Methods, Results, and Prospects), Moscow: Nauka, 1989, pp. 209–227.

Nikonov, A.I., Tectonophysical aspects of structural deciphering of lineament structures, *in Sovremennaya tektonofizika: metody i rezul'taty. T. 2* (Modern Tectonophysics: Methods and Results), Moscow: IFZ RAN, 2011, vol. 2, pp. 78–93.

Osokina, D.N. *Plastichnye i uprugie nizko-modul'nye optcheski-aktivnye materialy dlya issledovaniya napryazhenii v zemnoi kore metodom modelirovaniya* (Ductile and Elastic Low-Module Optically Active Materials for Modeling Stress in the Earth's Crust), Moscow: AN SSSR, 1963.

Paleoseismologiya (Paleoseismology), McCalpin, J.P., Ed., Amsterdam–Boston–Heidelberg: Academic Press, 2009.

Petrov, V.A., *Tektonofizicheskie usloviya formirovaniya VTS Vostochno-Zabaikal'skoi uranovorudnoi provintsii* (Tectonophysical Conditions of Formation of the VTS Eastern Transbaikalian Uranium Province), Moscow: IGEM RAN-VIMS, 2007, pp. 140–144.

Petrov, V.A., Andreeva, O.V., and Poluektov, V.V., "Effect of petrophysical properties and deformation on vertical zoning of metasomatic rocks in U-Bearing volcanic structures: a case of the Strel'tsovka Caldera, Transbaikal Region," *Geol. Ore Deposits,* 2014, vol. 56, no. 2, pp. 95–117.

Petrov, V.A., Rebetsky, Yu.L., Poluektov, V.V., and Burmistrov, A.A., "Tectonophysics of Hydrothermal Ore Formation: an Example of the Antei Mo–U Deposit, Transbaikalia," *Geol. Ore Deposits,* 2015, vol. 57, no. 4, pp. 292–312.

Petrov, V.A., Sim, L.A., Nasimov, R.M., and Shchukin, S.I., Fault tectonics, neotectonic stresses, and hidden uranium mineralization in the area adjacent to the Strel'tsovka Caldera, *Geol. Ore Deposits,* 2010, vol. 52, no. 4, 279–288.

Pogorelov V.V., Koneshov V.N., and Rebetsky, Yu.L., Numerical modeling of strains in the western flank of the Zond subduction zone, *Vestn. KRAUNTs. Nauki o Zemle*, 2010, vol. 15, no. 1, pp. 174–192.

Rasskazov, I.Yu., Saksin, B.G., Petrov, V.A., et al., Present-day stress-strain state in the upper crust of the Amurian lithosphere plate, *Izv. Phys. Solid Earth,* 2014, vol. 50, no. 3, pp. 444–452.

Rasskazov, I.Yu., Saksin, B.G., Petrov, V.A., and Prosekin, B.A., Geomechanical conditions and specifics of dynamic manifestation of rock pressure at the Antei deposit, *Fiziko-Tekhn. Probl. Razrab. Polezn. Iskop.,* 2012, no. 3, pp. 3–13.

Rebetsky, Yu.L., *A review of methods of reconstruction of tectonic stress and seismotectonic strains, Tectonophysics Today,* Moscow: OIFZ RAN, 2002, pp. 227–243.

Rebetsky, Yu.L., Methods of tectonophysical reconstruction of stress and strains in natural massifs using geological and seismological indicators, *Sovremennaya tektonofizika: Metody i rezul'taty* (Modern Tecctonophysics: Methods and Results), Moscow: *IFZ RAN*, 2011, vol. 2, pp. 109–146.

Rebetsky, Yu.L., Features of stress state of the crust of intracontinental orogens, *Geodinam. Tektonofiz.,* 2015, no. 4, pp. 437–466.

Rebetsky, Yu.L. and Kuzikov, S.I., Active faults of the northern Tien Shan: tectonophysical zoning of seismic risk, *Russ. Geol. Geophys.,* 2016, no. 6, pp. 1225–1250.

Rebetsky, Yu.L. and Lermontova, E.S., *On long-range influence of regions of anomalous stress state for medium in a supercritical state, Aktivnye razlomy i ikh znachenie dlya otsenki seismicheskoi opasnosti: sovremennoe sostoyanie problem* (Active Faults and their Significance for Assessment of Seismic Hazard: Modern State of the Problem), Voronezh: Nauchnaya Kniga, 2014, pp. 331–337.

Rebetsky, Yu.L., Sycheva, N.A., Kuchay, O.A., and Tatevossian, R.E., Development of inversion methods on fault slip data. Stress state in orogenes of the Central Asia, *Tectonophysics,* 2012, vol. 581, pp. 114–131.

Reinecker, J., Heidbach, O., Tingay, M., et al., The 2005 Release of the World Stress Map. www.world-stress-map.org

Romanyuk, T.V., Vlasov, A.N., Mnushkin, M.G., et al., Rheological model and features of stress-strain state of the active strike-slip fault zone by the example of the San-Andreas fault. Paper 1. San-Andreas Fault as a tectonophysical structure, *Byull. Mosk. O-va Ispyt. Prir., Otd. Geol.,* 2013, vol. 88, no. 1, pp. 3–19.

Rybalov, B.L., Spatial distribution of Late Mesozoic ore deposits in the eastern Transbaikal Region (Russia), *Geol. Ore Deposits,* 2002, vol. 44, no. 4, pp. 312–323.

San'kov, V.A., Levi, K.G., Kale, E., et al., Modern and Holocene horizontal movements on the Baikal geodynamic test site, *Geol. Geofiz.,* 1999, vol. 40, no. 3, pp. 422–430.

San'kov V.A., Levi K.G., Lukhnev A.V., and Miroshnichenko, A.I., *Present-day movement of lithospheric blocks of Central Asia: GPS-geodetic data, Aktual'nye voprosy sovremennoi geodinamiki Tsentral'noi Azii* (Actual Problems of Modern Geodynamics of Central Asia) Levi, K.G. and Sherman, S.I., Eds., Novosibirsk: SO RAN, 2005, pp. 165–179.

Seminskii, K. Zh., Kozhevnikov, N.O., Cheremnykh, A.V., et al., Interblock zones in the crust of the southern East Siberia: tectonophysical interpretation of geological–geophysical data, *Geodinam. Tektonofiz.,* 2013, vol. 4, no. 3, pp. 203–278.

Sherman, S.I., Natural trigger mechanisms of disturbance of metastable state of fault-block medium of lithosphere in real time, *Fiziko-tekhnicheskie problemy razrabotki poleznykh iskopaemykh* (Physico-Technical Problems of Development of Mineral Resources), Novosibirsk: SO RAN, 2009, no. 5, pp. 33–48.

Sim, L.A., Study of tectonic stresses using geological indicators: methods, results, and recommendation, *Izv. Vyssh. Uchebn. Zaved. Geol. Razved.,* 1991, no. 10, pp. 3–22.

Sim, L.A., *Application of field methods for reconstruction of tectonic stresses using fault data for solution of theoretical and practical tasks, Sovremennaya tektonofizika: Metody i rezul'taty* (Modern Tectonophysics: Methods and Results), Moscow: IFZ RAN, 2011, vol. 2, pp. 156–171.

Sim, L.A., A brief review of investigations of paleotecctonic stresses and their significance for solution of geodynamic problems, *Geodinam. Tektonofiz.,* 2013, no. 4, pp. 341–361.

Solov'ev, N.S., Shatkov, G.A., Yakobson, L.N., et al., Argun–Mongol volcanic belt, *Geol. Geofiz.,* 1977, no. 3, pp. 20–31.

Stefanov, Yu.P., Numerical modeling of Deformation and Destruction of Geological Media, *Extended Abstract of Doctoral (Geol.-Min.) Dissertation,* Tomsk: 2008.

Urbancic, T.I. and Trifu, C.-I., Shear zone stress release heterogeneity associated with two mining-induced events of M 1.7 and 2.2, *Tectonophysics,* 1998, vol. 289, pp. 75–89.

Vlasov, A.N., Yanovskiy Yu.G., Mnushkin, M.G., and Popov, A.A., *Solving geomechanical problems with UWay FEM package, Computational Methods in Engineering and Science, Iu, V.P.*, Taylor and Francis, 2004, pp. 453–461.

Voitenko, V.N., Model of formation of folds in the central Talas Alatau: data of microstructural and strain analysis, *Vestn. St. Peterb. Gos Univ., Ser. 7,* 2000. vol. 4, no. 31, pp. 78–84.

Voitenko, V.N., Correlation of parameters of finite stresses and anisotropy of magnetic susceptibility: comparison of results of study of metaturbidites of northwestern Ladoga region, *Tektonofizika i aktual'nye voprosy nauk o Zemle* (Tectonophysics and Actual Problems of the Earth's Science), Moscow: *IFZ RAN*, 2008, vol. 1, pp. 22–25.

Voitenko, V.N., Pogorelov, V.V., Yakubovskaya, A.O., and Goneger, A.V., Modeling stress and strain fields with allowance for evolutionary formation of geostrucures: evidence from the Sailag Massif, East Sayan, *Geodinam. Tektonofiz.,* 2013, no. 4, pp. 419–433.

Vol'fson, F.I., Ishchukova, L.P., Vishnyakov, V.E., et al., Conditions of localization of hydrothermal uranium mineralization in the stratified sequences of the upper structural stage, *Izv. Aakad. Nauk SSSR, Ser. Geol.,* 1967, no. 11, pp. 114–134.

Yunga, S.L., *Metody i rezul'taty izucheniya seismotektonicheskikh deformatsii* (Methods and Results of Study of Seismotectonic Deformations), Moscow: Nauka, 1990.

Zhirov, D.V., Sim, L.A., and Marinin, A.V., *Reconstruction of the paleostress-state in the southern Khibina Pluton (eastern Fennoscandian Shield), Aktual'nye problemy dinamicheskoi geologii pri issledovanii platformennykh oblastei* (Actual Problems of Dynamic Geology during Study of Platform Areas), Moscow: MGU, 2016, pp. 39–44.

Translated by V. Popov